CHAPTER 8

MORPHOLOGY OF INDIVIDUAL THUNDERSTORMS AND ATTENDANT PHENOMENA

8.1 Thunderstorm Cells and Their Evolution. Refer to Part D, Chapter 4, of this Handbook for operational application of the WSR-88D to convective and severe convective storms which also contains a discussion of the critical velocity signatures and morphology associated with severe convective storms. The following discussion applies primarily to the distribution, character, and changes in the water substance within convective storms via detection by radar.

The dynamical building block of a thunderstorm is the cell. A cell is a compact region of relatively strong vertical air motion (many meters per second). With radar, cells are identified by their associated volumes of precipitation.

Most thunderstorms are composed of several short-lived cells known as ordinary cells. At any given time, such storms consist of a succession of ordinary cells at different stages of evolution. There are three stages in the evolution of ordinary cells (Figure 8-1): cumulus, mature, and dissipating.

The cumulus stage is characterized by updrafts throughout the cell. As the cell builds upward, moisture condenses and precipitation particles grow. The precipitation begins descending within the cloud and an associated downdraft begins to develop. This downdraft is forced by: 1) the drag exerted on the air by the precipitation particles and 2) negative buoyancy due to evaporational cooling as cloud and some of the condensate evaporates in dryer air that has been entrained into the storm from outside. The downdraft signifies the beginning of the mature stage.

The mature stage is characterized by precipitation reaching the ground. Updraft and downdraft coexist side by side, the downdraft being best developed in the lower portions of the precipitation shaft. With increasing downdraft development, cloud and more of the descending precipitation evaporates resulting in much of the downdraft displaced adjacent to, but outside of, the visual cloud. The downdraft brings evaporatively cooled air in the rain area toward the ground, where it produces a diverging pool of cold air. The leading edge of the cold air forms a micro cold front called a “gust front,” characterized by a sudden onset of shifting and gusty cool winds and rising pressure. New cells tend to form above and along this outflow.

The cell enters the dissipating stage when the updraft is replaced by downdraft, which spreads throughout the entire cell before weakening and disappearing. Simultaneously, the cold dome of downdraft air near the surface continues to spread outward becoming increasingly shallow and the winds behind the gustfront decrease. At this point, all that is left of the original cumulonimbus is often an “orphan anvil.” In other words, only the anvil aloft remains and the lower level cumulus cloud has dissipated.

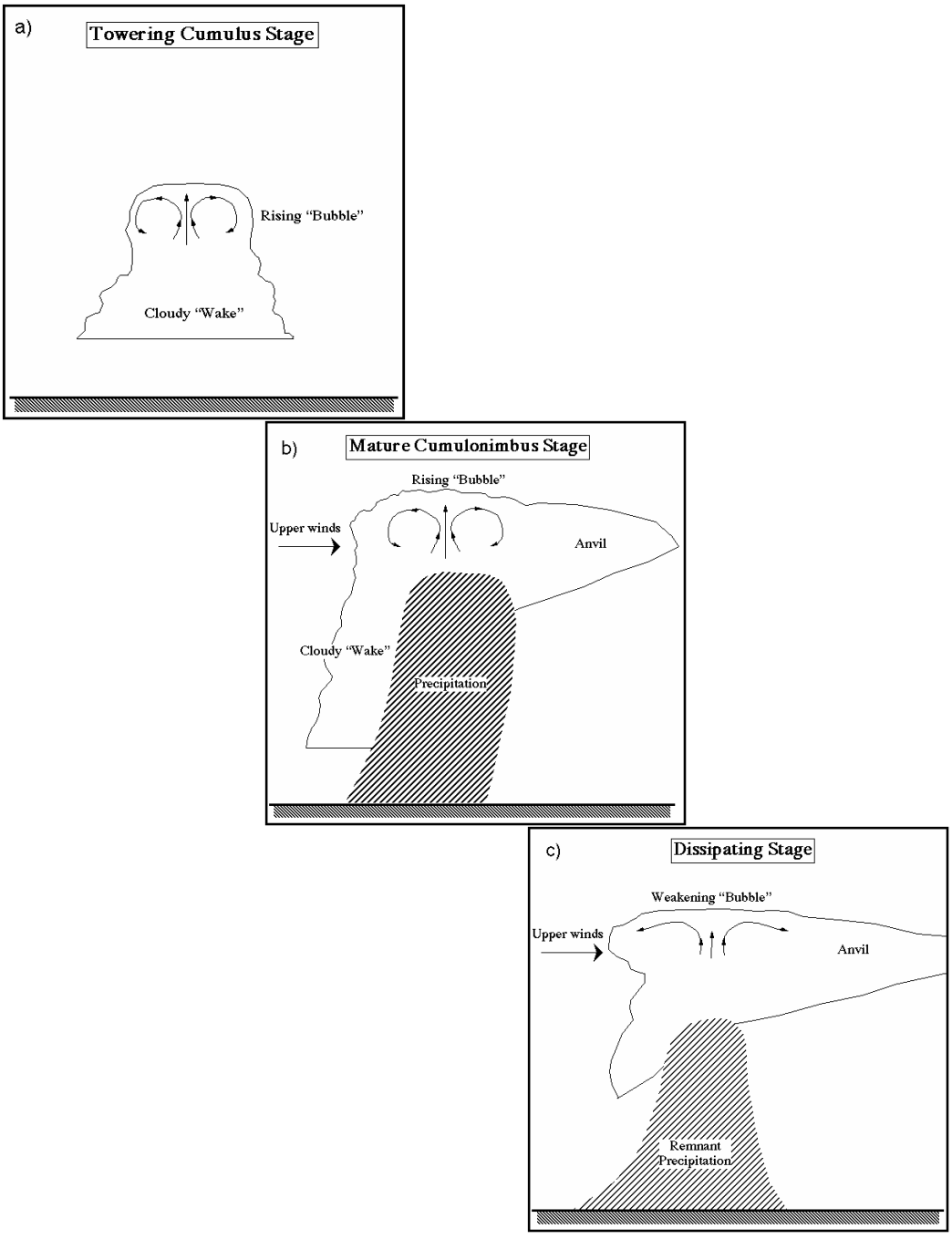

Figure 8-1
Ordinary Cell

The three stages of an ordinary cell life cycle, a) towering cumulous, b) mature, c) dissipating. Features of the figure are labeled showing distributions of cloud (outlined) encompassing updraft and precipitation encompassing downdraft. (From Doswell 2001, after Byers and Braham 1949).

The lifetime of an individual cell averages about 40 minutes, during which it may travel about 15 to 30 km (8 to 16 nm) in the general direction of the mean upper winds in which it is embedded. A storm consisting of a sequence of several such cells may, however, persist for several hours.

In the presence of considerable atmospheric instability and vertical shear of the horizontal wind, an extremely vigorous unit of convection known as a supercell may develop (Figures 8-2a through c). Supercells are relatively uncommon, evolve only slowly, and are often multicellular but dominated by a single large cell. These storms tend to be large, often 20 to 30 km (11 to 16 nm) or more in diameter. They are long-lasting (sometimes up to 6 or more hours) and cause a disproportionate amount of severe weather such as very large hail, damaging winds, and are often consistent tornado producers. Radar features of supercells are described in Section 8.5.4. The supercell's basic distinguishing feature is a deep, persistent "mesocyclone" in which vertical velocity and vertical vorticity are correlated, with vorticity magnitude of $\sim 1 \times 10^{-2}$ s^{-1} or greater within such a storm (e.g., Klemp 1987). Thus, significant vorticity is present within the updraft and perhaps the "Rear Flank Downdraft" (RFD). At times the RFD is a significant portion of the mesocyclone. The mesocyclone is seen as cyclonic shear in the radial velocity pattern (Figure 8-2a). (Note the bright red color coded velocity adjacent to the bright green.) Additionally, the air circulation is only slowly evolving, with updraft and downdraft coexisting in a symbiotic manner for long periods. Essentially, the supercell is a prolonged version of the mature stage of an ordinary cell, but with the addition of the mesocyclone in which the updraft-downdraft couplet takes on a stable and mutually beneficial configuration.

Unlike ordinary cells that tend to drift with the cloud-bearing winds, supercells travel with motion significantly different from the mean wind in the atmospheric layer that contains them, often moving markedly to the right or left of the mean wind.

In some cases and at times, without a Doppler radar, an observed cell may be difficult to classify as either an ordinary cell or supercell because there is not always a clear-cut and easily determined distinction within the reflectivity field. For further detail concerning severe convective storms, the reader is referred to Browning (1977), Lemon and Doswell (1979), Doswell and Burgess (1993), and Doswell (2001) as well as many of their references.

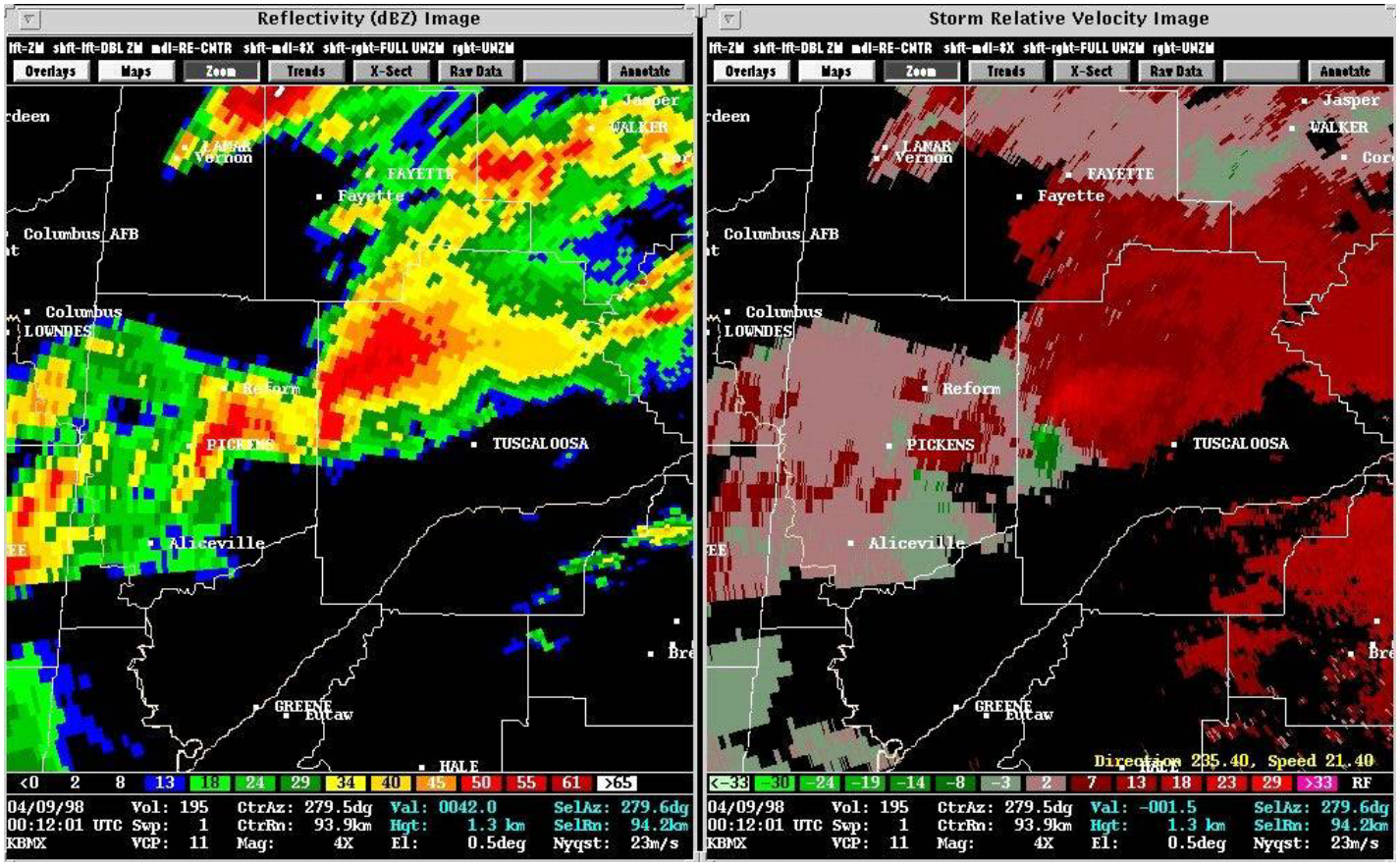

Figure 8-2a
Doppler Radar Display of a Supercell at a Low Elevation

Seen here (storm in display center) is a mature supercell storm northwest of Tuscaloosa, AL, at 00:12 UTC on 8 April 1998 as scanned by the Birmingham, AL WSR-88D (WDSS display). Left display provides a view of the reflectivity field and the right, the Mean Radial Velocity. The velocity color code is in knots with the red colors signifying flow moving away from the radar and flow approaching the radar in green. Brighter colors are higher velocities. The color changes abruptly from red to green at the storm's right rear marks the position of the mesocyclone.

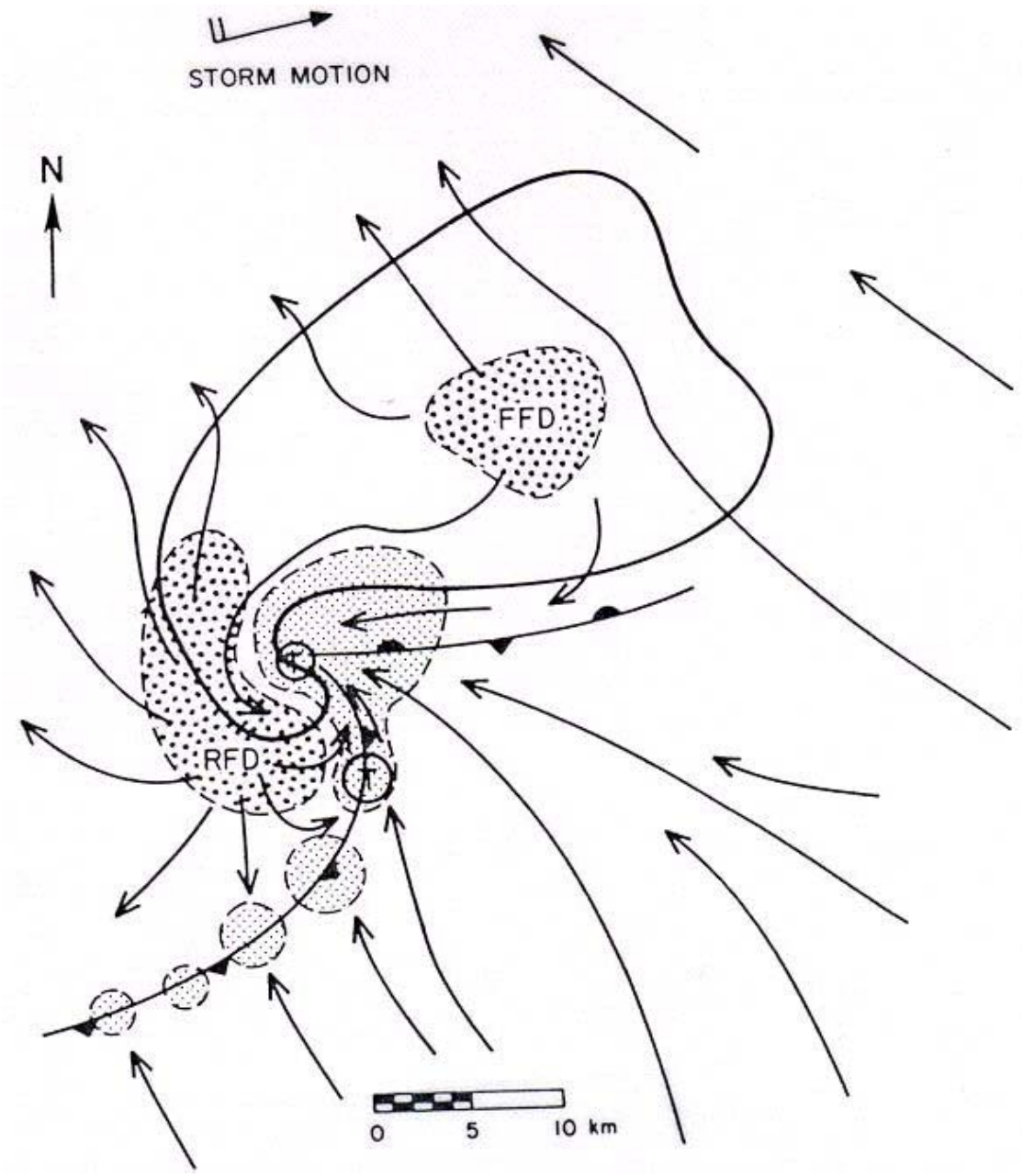

Figure 8-2b
Schematic Plan View of an Isolated Classic Supercell Storm Near the Surface

Thick line encompasses radar echo (note hook on southwest side). The wave-like gust front structure, resembling a synoptic scale cyclone, is depicted by classical frontal symbols and is part of the mesocyclone circulation. Low-level positions of the updraft and forward flank downdraft (FFD) and rear flank downdraft (RFD) are shown. Favored locations for tornadoes are near mesocyclone center (T) and along bulge in “pseudo-cold" front. Thin arrows depict storm-relative streamlines. (Adapted from Lemon and Doswell 1979).

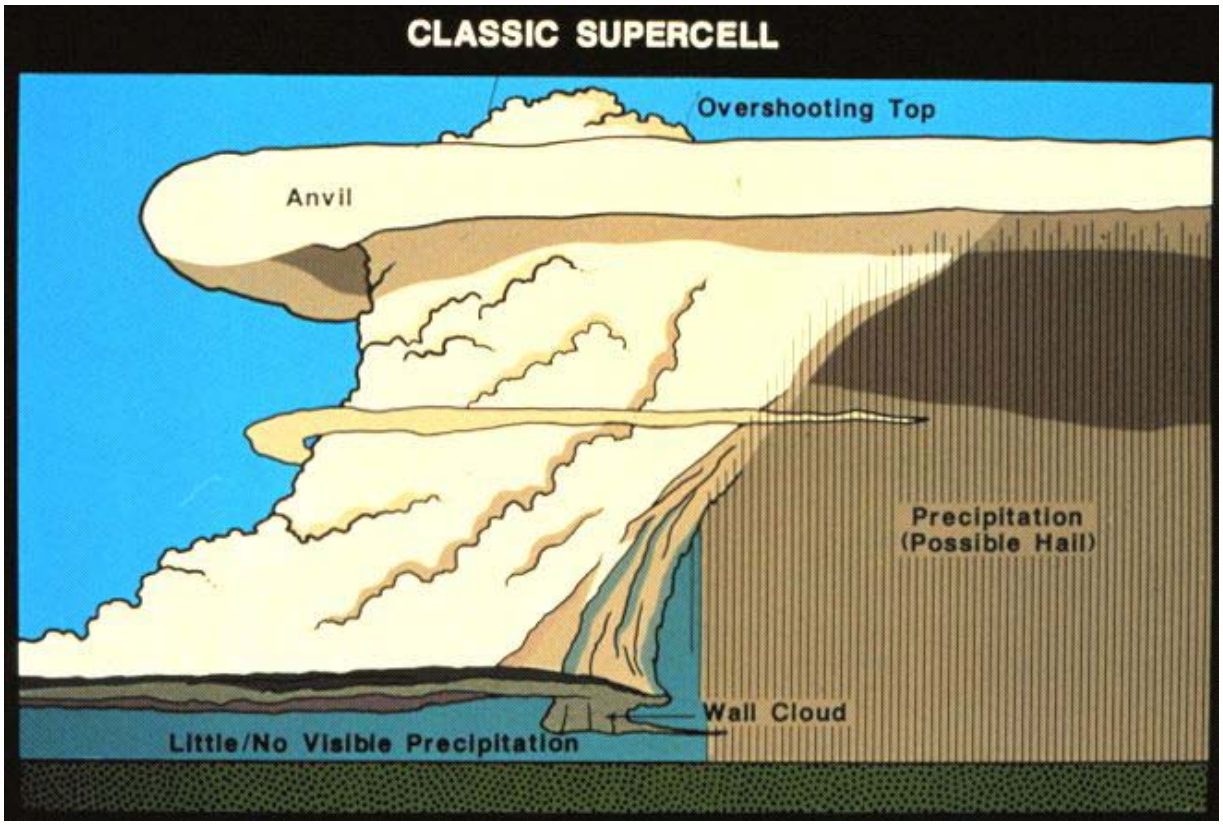

(Reproduced/modified by permission of American Geophysical Union.)

Figure 8-2c
Vertical View of Typical Classic (Supercell) Tornado-Producing Cumulonimbus

As seen from a southeasterly direction. Horizontal scale is compressed. All the features shown cannot be seen simultaneously from a single direction. Shelf cloud may not be present or may be to the left of the wall cloud. With time, spiral precipitation curtain wraps cyclonically around wall cloud from right to left. (From Doswell and Burgess 1993)

8.2 Types of Thunderstorms. In this document as in the science, we attempt to classify storms by storm "type." Over the years there have been attempts to develop a thunderstorm taxonomy such as that which began with the thunderstorm project of Byers and Braham (1949). Other attempts, Marwitz (1972) and Browning (1977), built upon the early "cellular" convection concept and further expanded it. This has been done in order to facilitate our convective storm understanding and to better discuss these storms in a meaningful and more utilitarian manner. But these taxonomies are conceptual in nature and should not be taken too literally or dogmatically. Real storms resist being placed in orderly and neat bins or categories. As will become clear, these conceptual models tend to deal with the degrees of draft steadiness and strength, especially the updraft. In some cases the updraft is seen as a "bubble" of weakly rising air and in other cases as a more-or-less steady and strong current. In reality there is probably a continuum ranging from the bubble at one end and the steady current at the other end of a broad spectrum. Furthermore, in reality there is a broad convective storm spectrum ranging from the single ordinary cell or storm at one end to the multicell, and finally to the true, quasi-steady state supercell. Moreover, this spectrum of storms is continuous in nature with categories considerably blurred and blended. In the study of convective storms we have somewhat arbitrarily chosen to divide this spectrum into individual categories. That is what has been done in this Handbook. The reader is reminded that reality will support these conceptual models only so far.

Browning (1977) introduced the storm classification system that consisted of basically two types of convective storms, the ordinary, and the supercell (Figure 8-3). However, for our purposes, we will also retain certain portions or aspects of the standard classification of Marwitz (1972) and divide thunderstorms into three basic categories as follows:

1. The supercell storm. It consists of one dominant cell (often with smaller cells embedded within the echo) that includes cyclonic (anticyclonic) turning of the mid-level updraft, i.e., the deep, persistent mesocyclone (mesoanticyclone) and continuously propagates to the right (left) of the mean winds. It often progresses steadily but slowly through a somewhat predictable evolution (Lemon and Doswell 1979; Burgess et al. 1982; Dowell and Bluestein 2000, 2002a) for 1 to 6 hours, or more (Figures 8-2a through c). A sub-classification is often recognized that includes the "Classic" (CL), the "Heavy Precipitation (HP), and the Low Precipitation (LP) supercell storms (Moller et al. 1990).

2. The multicell storm. It consists of several ordinary cells, and propagates discretely as new cells develop and old cells dissipate, sometimes in an organized fashion (Figure 8-4a, b).

3. The squall line. It consists of ordinary cells and sometimes supercells that are arranged in a linear fashion (Figure 8-5). Squall lines and MCS's are discussed somewhat in Section 8.5.7 and in Part B, Chapter 7, of this Handbook.

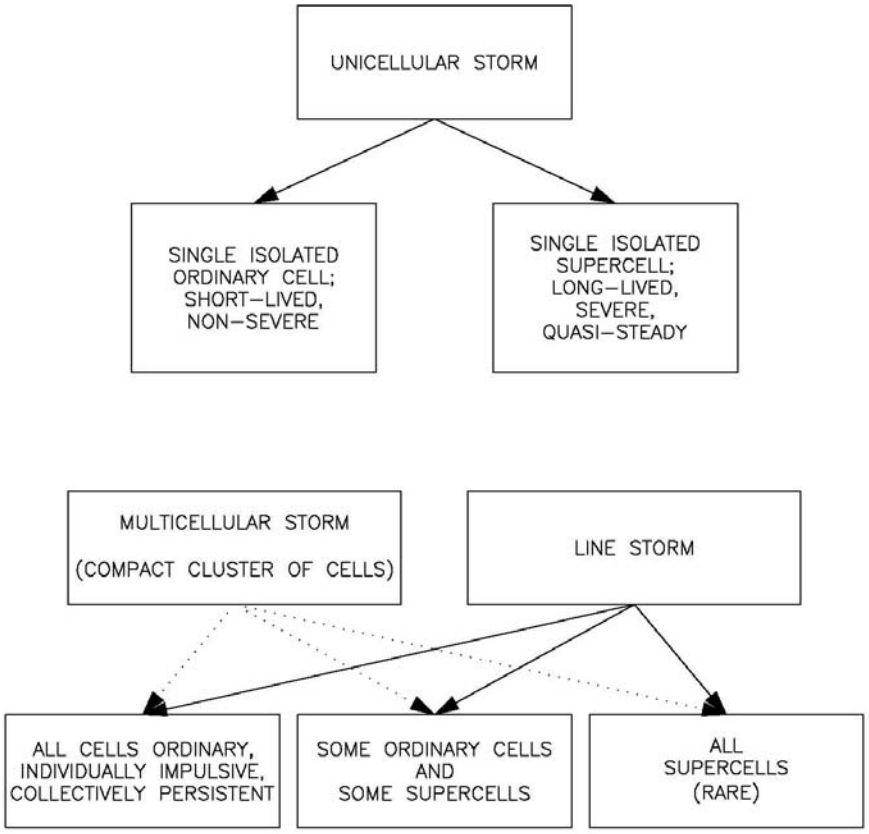

Figure 8-3
Browning's Classification of Thunderstorm Types

(From Browning 1986).

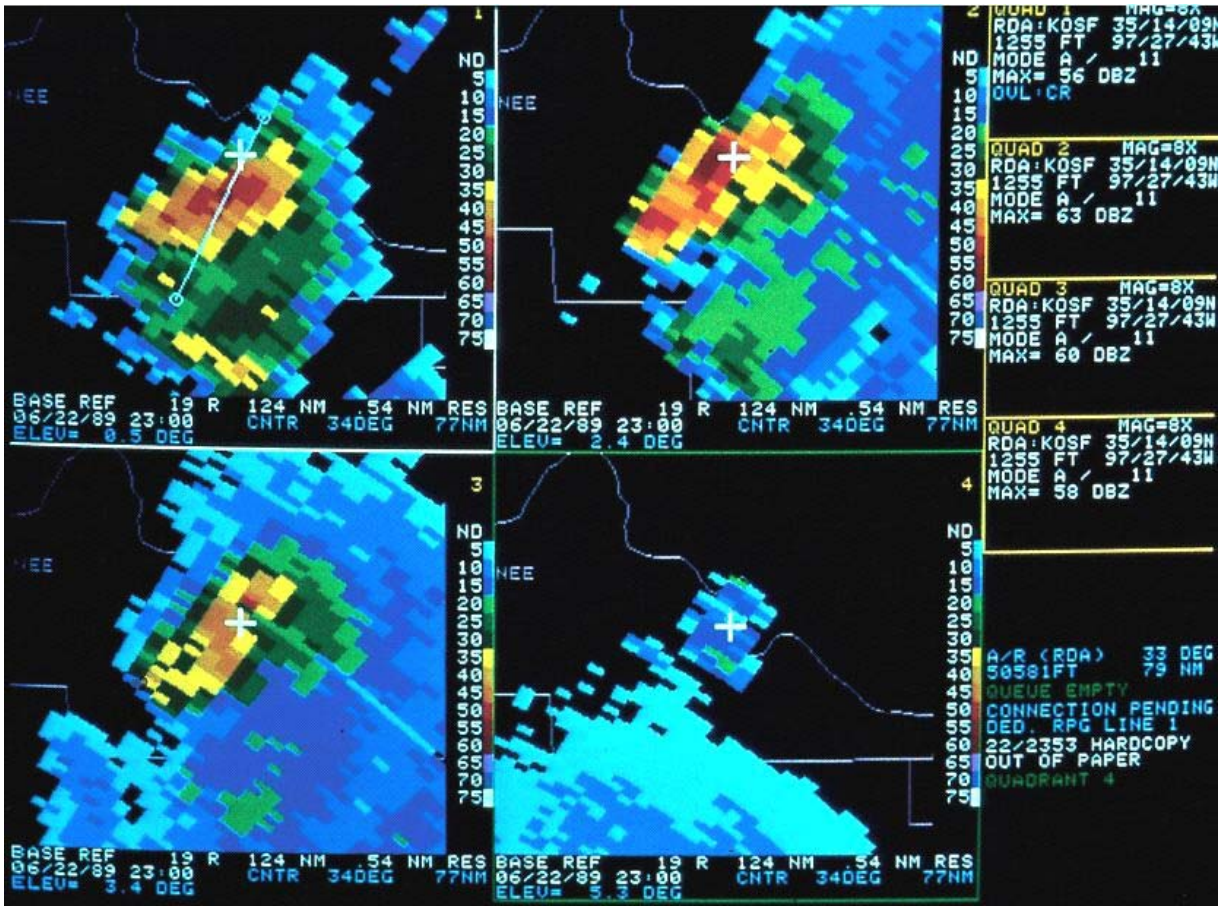

Figure 8-4a
Display of a Multicell Storm (4 - Panel)

An Oklahoma City, OK WSR-88D quarter screen Reflectivity product display of a multicell storm (PUP display) at 23:00 UTC on 22 June 1989. The magnified product elevations are as follows: upper left, 0.5°, upper right 2.4°, lower left, 3.4°, and lower right, 5.3°. Note the vertical cross section axis overlaid on the echo in the upper left quadrant or quadrant 1 (see Figure 8-4b). The white cross is at the same geographical location in all four panels.

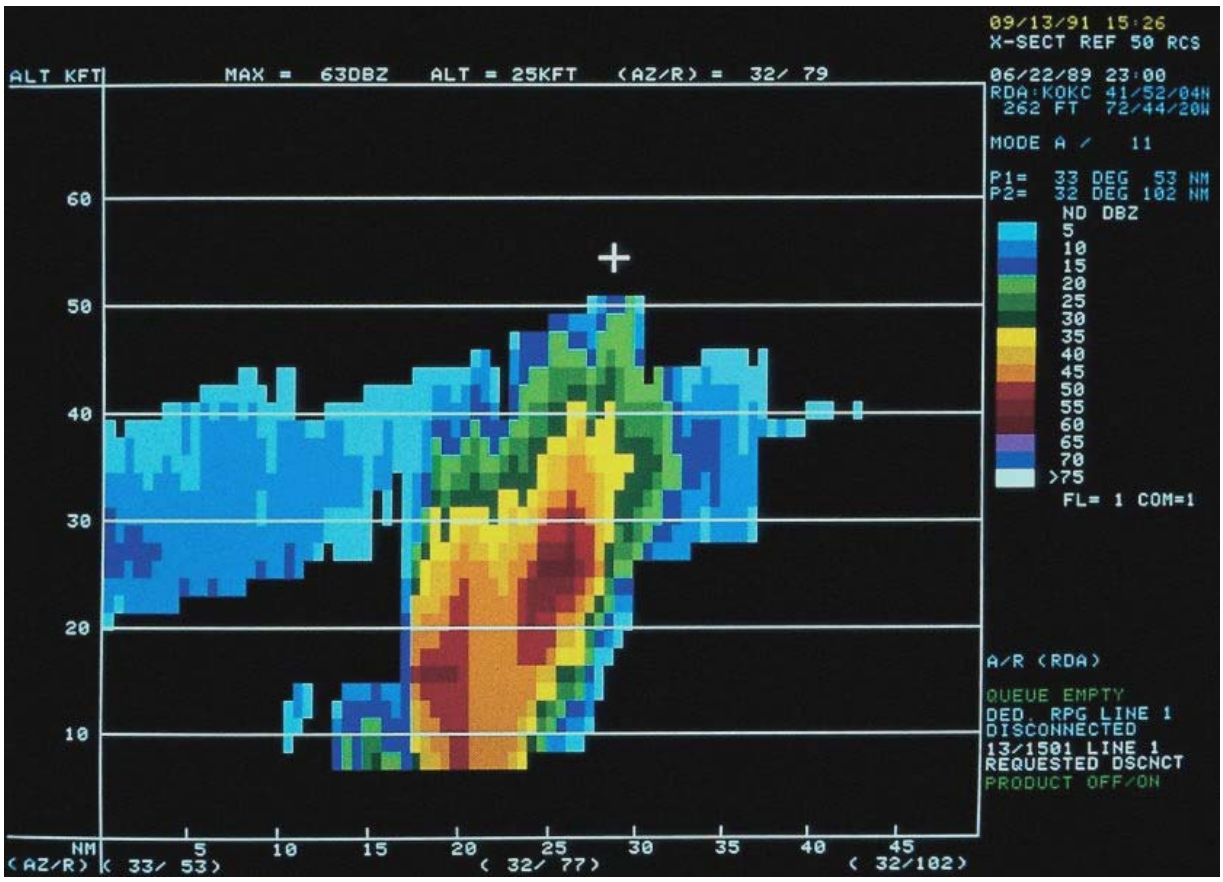

Figure 8-4b
Display of a Multicell Storm (Vertical Cross Section)

The Reflectivity (vertical) Cross Section along the axis shown in Figure 8-4a showing the structure of this multicell storm (PUP display).

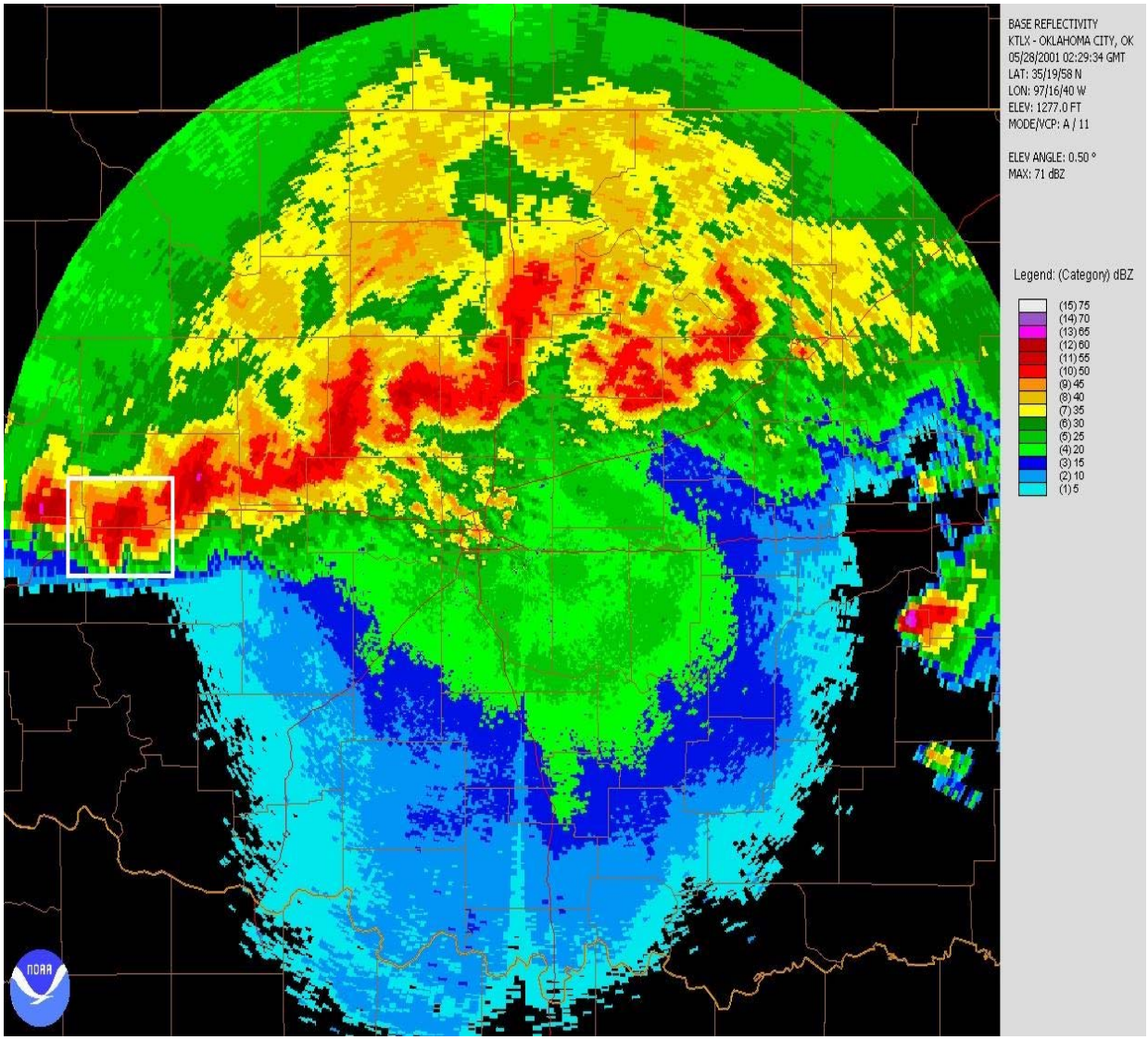

Figure 8-5
Display of a Squall Line at Low Elevation Angle

This line of thunderstorms consisted of both supercells and ordinary cells. This image os from the Oklahoma City, OK WSR-88D at 02:29 UTC on 28 May, 2001 (NCDC NEXRAD Viewer graphic). Note one of the supercells enclosed in the white box west of the radar. Reflectivity data levels are as labeled.

Browning (1986) points out some weaknesses of the above scheme; in particular, both multicell storm clusters and squall lines may contain supercells. Browning prefers the following classification (Figure 8-3).

1. Unicellular storm (e.g., Figures 8-1, 8-2a through c).

2. Multicellular storm (with a cluster of cells, not forming in a distinct line, such as in Figures 8-4a, b).

3. Line storm, i.e., squall line (containing cells along a line as in Figure 8-5).

Unicellular storms may consist theoretically of either a single ordinary cell of short duration or ideally, a supercell of long duration. (True unicellular storms, whether ordinary or supercell, are likely very rare if they do actually occur at all in nature.) Unicellular supercell storms are generally referred to simply as supercell storms (ignoring any multicellular characteristics that might be present). Multicell clusters and line storms may contain all ordinary cells, a mixture of ordinary and supercells, or (rarely) all supercells (Figure 8-5). Most supercell storms start and end life as none severe evolving multicellular storms.

8.3 Environmental Factors Governing Storm Type. Supercells form when the environmental deep layer vertical wind shear (horizontal vorticity) reaches a critical range such that it can be tilted into the vertical and stretched by strong thunderstorm updrafts supported by sufficient thermal instability (Klemp 1987; Johns et al. 1993) (Figure 8-6). Storms are weak when the instability and shear are slight. When the instability is high but the shear is low, storms consist of ordinary cells that are sometimes strong for short time-periods, either in isolation (the "pulse storm") or in disorganized multicellular clusters. Strong shear and weak instability can lead to supercell storms that are sometimes called "severely sheared" storms and/or short lived ordinary cells.

When the shear and thermal instability are both moderate or strong, the storms that develop tend to be well organized, supercells, multicell clusters, or squall lines and can produce very severe weather. Given that convective storms will occur with sufficient instability and deep layer shear (generally seen as shear from the surface to 6 km AGL) of greater than about 15-20 ms^{-1} (~30-40 kts), then supercells are the favored mode of organized convection and often produce very severe weather (Figure 8-6). With insufficient shear, storms are likely to be less organized multicell clusters or line storms, depending on whether the atmospheric mechanism that triggers the storms is confined to a local area or linear, such as along a dryline or front.

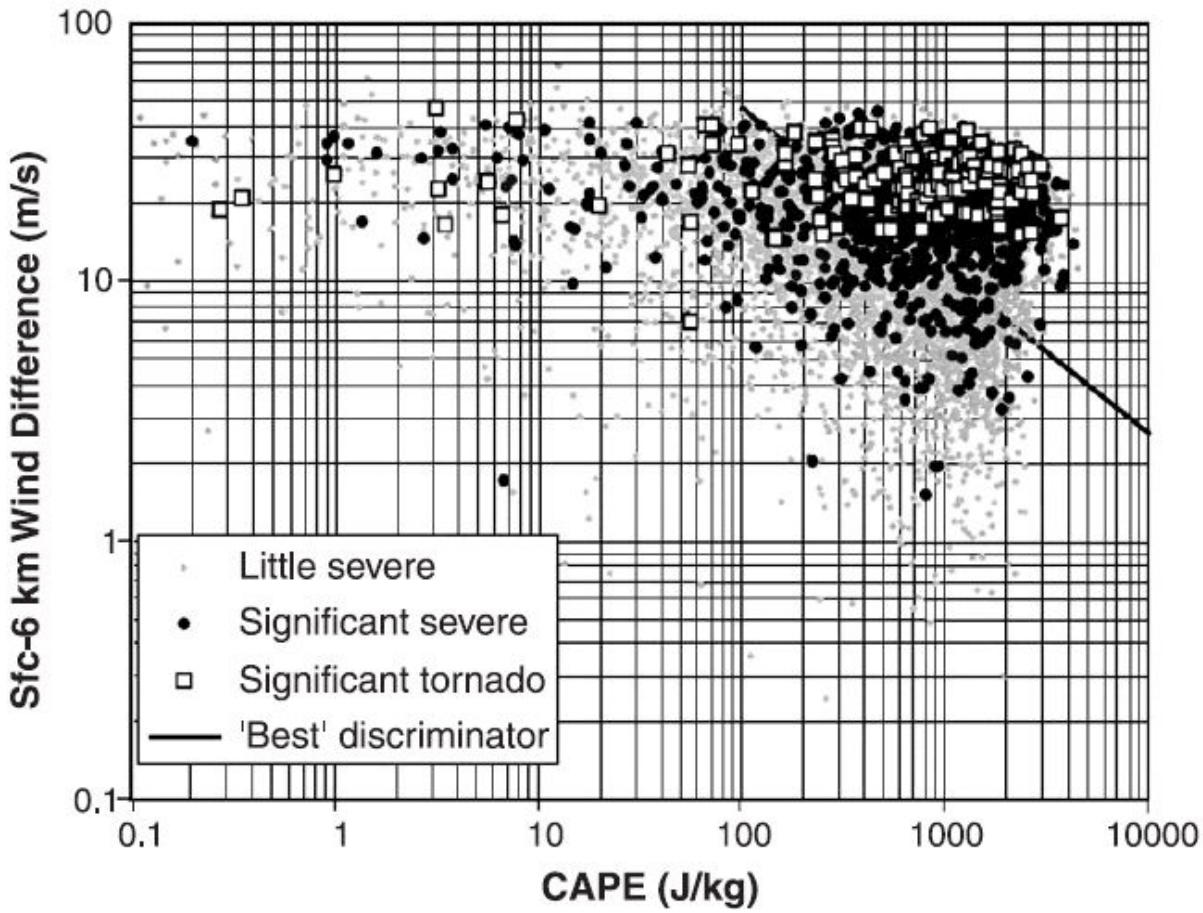

Figure 8-6
Surface to 6 km Wind Difference Versus CAPE

Magnitude of the vector wind difference (shear) between the surface and 6 km (ms^{-1}) and CAPE ($J\ kg^{-1}$) for all reanalysis soundings associated with severe thunderstorms in the US for 1997– 1999, segregated by weather type: non-significant severe weather (small gray dots), significant, non-tornadic severe weather (large black dots), and significant tornadoes (open squares). Solid black line is best discriminator between soundings associated with significant severe thunderstorms of any kind and other soundings. Note that non-severe soundings are not included in the figure. From Brooks et al. (2003).

As storms develop along a linear discontinuity, such as a boundary, and if the deep-layer shear vector tends to parallel the boundary, then adjacent storms interfere with one another such that precipitation from the up-shear storm will fall within (or seed) the down-shear storm. This typically leads to quasi-linear, two-dimensional, or continuous squall lines with few, if any breaks in the line. On the other hand, if the shear vector tends to be oriented more normal or perpendicular to the boundary, then individual storms will tend to be more isolated leading to scattered or broken lines of storms. If both instability and shear are sufficient, these individual storms developing within the line have a better chance of becoming supercells. Due to storm evolution, local meteorological conditions, and terrain effects, the dominant storm type may change over short distances and times.

Obviously, greater thermal instability means more potential energy available for storms to convert into kinetic energy and strong updrafts. The presence of dry air at mid-levels contributes to this available energy because it favors more intense downdrafts through increased evaporative cooling.

Shear has an important effect on storms for several reasons. First, precipitation is carried away from the updraft and allowed to cascade into the downdraft region favoring coexistence of both updraft and downdraft. Thus the storm's updraft and downdraft may co-exist side-by-side in a stable symbiotic configuration for prolonged periods. Second, the resulting storm-relative winds favor sustained and augmented low-level inflow into the updraft. This also helps keep the gust front from moving out away from the storm. Further, the interaction between the sheared environmental winds and the storm updraft causes a dynamic pressure gradient to develop that favors updraft propagation on one flank of the storm and decay on the other flank. Third, the presence of favorable vertical shear (often veering winds with increasing height) creates low-level horizontal vorticity that can be aligned with storm-relative inflow and tilted into the vertical. This can also eventually develop from unidirectional but sheared flow. The result is creation of substantial vertical vorticity within the updraft. Supercell storms and strong tornadoes require this vital raw ingredient.

Let's consider the development of vorticity in a little more detail. As an updraft extends into a sheared environment, horizontal vorticity tilting acts to create two vertical "vortices" in storm mid-levels. (While sometimes we use the term "vortices" or "rotation," in actual fact we are speaking of enhanced vertical vorticity and not necessarily true, closed, vortices or rotation.) The strength of these vortices depends on the strength of the shear and the intensity of the updraft. Facing toward the direction of the shear, on the right side of the updraft lies enhanced cyclonic vertical vorticity or vortex while on the left is found enhanced anticyclonic vertical vorticity. Initially, the vortices lie along the periphery of the updraft, and thus contain little updraft within them. However, the presence of this enhanced mid-level vorticity on either flank creates dynamically driven low pressure coincident with these vortices, thus creating vertically directed upward motion on either side of an initial large updraft. With the dynamic pressure at its lowest aloft, this enhanced upward directed pressure gradient force promotes the development of new updraft within enhanced vorticity centers. The effect is a widening of the updraft, new updraft growing on the flanks, and increasing correlation between updraft and vorticity on both flanks. For more detail the reader is

encouraged to examine *Anticipating Convective Storm Structure and Evolution* and *A Convective Storm Matrix: Buoyancy/Shear Dependencies*. COMET (1996).

8.4 Storm Motion. Individual ordinary cells tend to move with the mean wind of the atmospheric layer that contains them (usually the entire troposphere). This is not surprising.

In a squall line, ordinary cells move roughly with the velocity of the mean wind, while the line as a whole moves roughly normal to its orientation and at a different speed. But this is understood since the motion of a two-dimensional feature can only be defined normal to its axis. Consider an example where the individual cells are arranged in a north-south line and cell motion is northeastward. Due to new cells developing on the southern end of the line and decaying on the northern end, the entire line moves eastward. Each individual cell is born at the southern tip of the line, moves up the line with time due to the organized pattern of birth and decay, and dies at the northern end.

Multicellular storm clusters (with all ordinary cells), in an environment with significant wind shear, have a similarly organized structure. The difference between individual cell motion and overall storm motion is again due to discrete cell and updraft propagation (Figure 8-7).

The motion of supercell storms also deviates from the mean wind. As explained above, interaction of the storm with the vertical shear profile generates a vertically directed dynamic pressure gradient force that continuously promotes new updraft on the flanks of the initial updraft. In addition, the manifestation of vertical vorticity within the mid-level updraft further promotes dynamic lift on the updraft flanks. The greatest tilting of horizontal vorticity occurs right and left of the shear vector. This means that the development of rotation and new updrafts also occur to the right and left of the shear vector. Precipitation developing in the middle of the widening updraft acts to develop a downdraft which, in turn, helps to split the widening updraft into two parts. The cyclonically (anticyclonically) rotating member moves to the right (left) of the shear vector. Since both the cyclonic and anticyclonic updrafts experience similar upward dynamic pressure forcing, they are equally strong supercells in a straight hodograph environment. The rightward deviating storm contains a cyclonic mesocyclone and the left deviating supercell or “left mover” contains an anticyclone or mesoanticyclone.

Once these supercells deviate off the hodograph, it experiences streamwise vorticity, and storm-relative helicity in its inflow layer. Tilting of the streamwise vorticity into the updraft immediately produces vertical vorticity well correlated with updraft. The processes that develop rotation in the unidirectional hodograph, also apply to curved hodographs. However, a curved hodograph implies that streamwise vorticity and helicity are available for the updraft to directly ingest upon its initial growth. In other words, the vorticity acts in the direction of the flow as in the thrown, spinning football. This represents the available streamwise vorticity that merely needs to be tilted into the vertical by the updraft in order for enhanced vorticity to be well correlated with the updraft. Therefore, the evolution from ordinary cell to supercell is much more rapid.

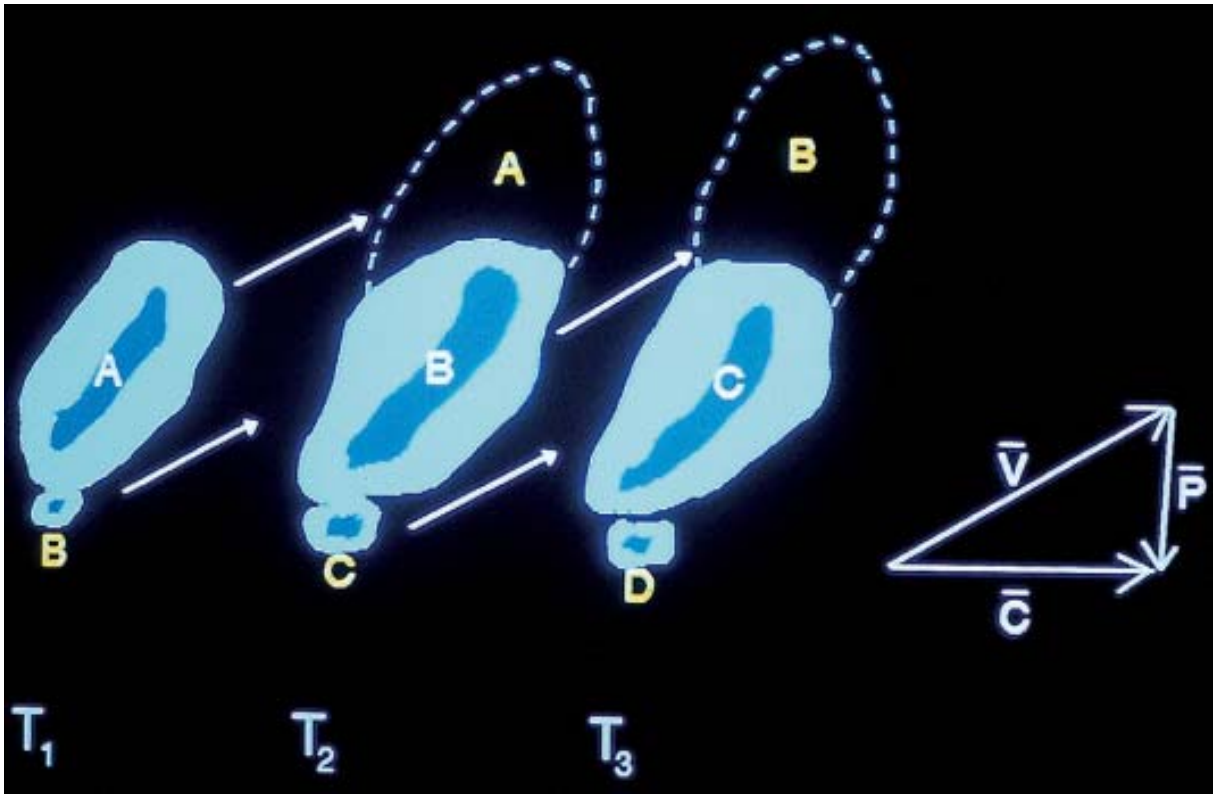

Figure 8-7
Conceptual Storm Motion Diagram

A schematic depicting storm motion where A – D are cells, V (bar) is cell advection, C (bar) is storm motion vector, and P (bar) is the propagation vector. Note that cells develop on the right flank, mature, and dissipate on the left flank in this example. However, there are almost an infinite number of variations, e.g., new development (propagation) may be occurring on the left forward flank with storm motion to the left of cell advection.

Finally, the presence of the gust front very near the edge of the precipitation cascade region and the RFD typically places it on the right rear storm flank (of the cyclonic supercell) where this further promotes boundary layer convergence. From there the gust front trails to the southwest or to the right rear of the mesocyclonic supercell storm. Thus, in the northern hemisphere, new updraft formation is strongly favored on the updraft flank, typically on the mesocyclonic supercell storm's right rear flank (especially for the Classic (CL)) and on the forward left flank of the left moving mesoanticyclonic supercell. The propagation is not only continuous, but it is often also discrete as new cells develop along the gust front and move into the storm complex. Thus, new updraft continuously, and often discretely, develop on the updraft flank strongly "driving" or "pulling" the storm significantly toward the updraft flank, on the right flank of the rightward deviating storm as compared to the prevailing environmental winds. The new growth on one side is balanced by decay in the region of downdrafts on the opposite side. Usually, mesocyclonic supercells move to the right of and slower than the mean wind while mesoanticyclonic supercells move to the left and faster than the mean wind. Such storms were originally called SR, Severe Right moving supercells by Browning (1964). As just explained, occasionally, SL, Severe Left moving supercells are observed. On those days when the vertical wind shear is strong and practically unidirectional, storms may split into SR and SL unidirectional supercells which follow highly divergent paths.

Therefore, and as explained above and by Klemp (1987), there is a close association between vertical vorticity within the updraft and anomalous motion, as exemplified by the mesocyclones (mesoscale anticyclonic circulations) observed in SR (SL) storms. For greater detail and illustration, the reader is encouraged to review *Anticipating Convective Storm Structure and Evolution* and *A Convective Storm Matrix: Buoyancy/Shear Dependencies*. COMET (1996).

8.5 Radar Reflectivity Structure of Thunderstorms. The three-dimensional reflectivity field of a storm's radar echo and its evolution contain a great deal of information about the storm's intensity and severe weather potential (tornado, hail, strong winds, turbulence).

8.5.1 Weak Echo Regions. An important concept in the interpretation of radar echoes is that of the WER associated with a strong updraft (Figure 8-8). The WER is created in part as a direct result of the updraft. A portion of the WER results when there is a sparsity of radar-detectable precipitation particles within the rapidly rising air in the updraft column. The echo weakness is due to the air rising so rapidly that precipitation does not have time to grow to detectability within the lower and mid-levels of the updraft. Additionally, precipitation formed elsewhere is unable to penetrate or fall through the updraft (Browning 1977).

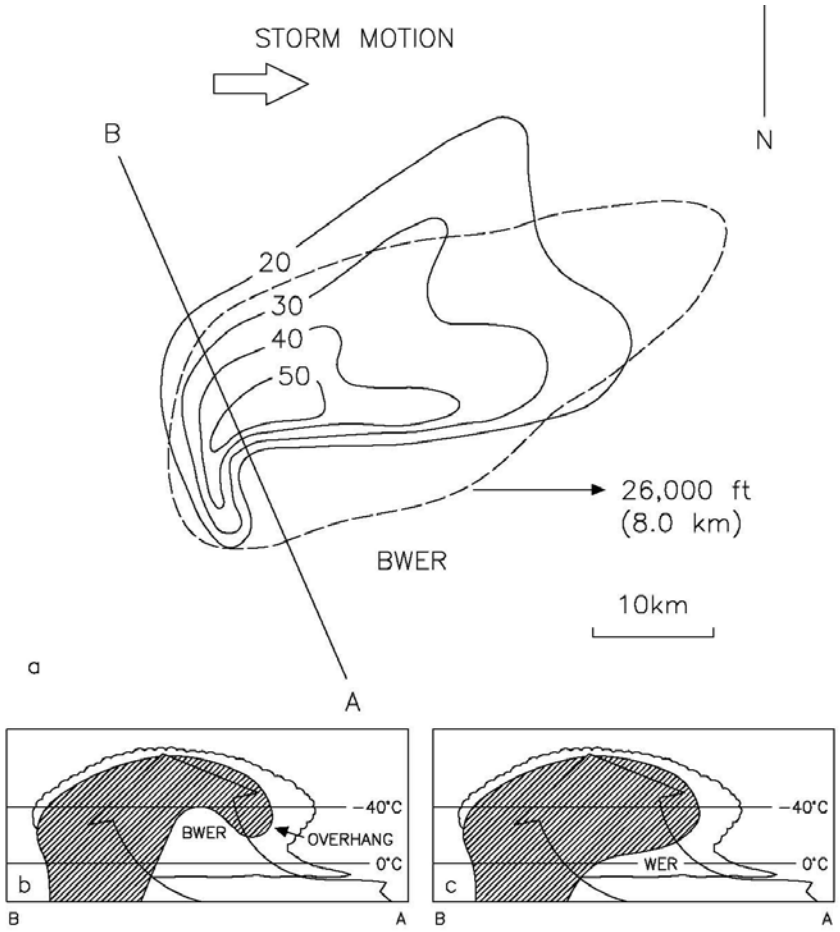

Figure 8-8
Schematic Diagrams Illustrating Bounded and Unbounded Weak Echo Regions

(a) Plan view of a right-moving supercell with a BWER. Solid lines are low-level and dashed lines are mid-level reflectivity in dBZ. Black dot is storm top (Lemon 1980). (b) Vertical cross section along line AB in (a). The extent of the radar echo (nominally 20 dBZ) is indicated by hatched shading and the location of the steady-state updraft and inflow is denoted by a bold arrow. Cloud outlines are also sketched (Browning 1977). (c) Vertical section along AB for a lesser developed storm than depicted in (a) and (b); here the weak echo region is unbounded.

However, the majority of the WER results when strong upper level divergence from the updraft summit transports large amounts of precipitation to high levels and is blown by the storm's relative winds (Lemon 1998). The result is a canopy of strong echo aloft with little or only weak echo beneath. As this precipitation descends from the cumuliform anvil aloft into the ambient environmental flow it forms what Browning termed the "slopping echo overhang." This should not be confused with the downstream anvil that may contain substantially weaker precipitation that evaporates as it descends but is still found aloft.

With increasing updraft (or sometimes as a result of better resolution at closer range), a bounded weak echo region (BWER) appears because air within the updraft core ascends still higher in the updraft before radar detectable precipitation particles form (Figure 8-8a). In a horizontal cross section, the weak echo region is completely surrounded, or bounded, by higher radar reflectivity values and results in the BWER. The acronym WER is reserved for unbounded weak echo regions (Figure 8-8b).

8.5.2 Ordinary Multicellular or Unicellular Storms in Weak Shear. The cumulus stage of each cell of an ordinary storm in weak shear begins on radar when the first echo develops aloft at temperatures between 0° C and -15° C or a height of 3 to 6 km (10,000 to 20,000 ft). The mature stage is marked by the tallest tops and highest reflectivities. The dissipating stage is associated with weakening reflectivities as the remaining precipitation developed aloft falls out. In the multicellular cluster, there are several cells at various stages of their life cycles. The complex of cells may last several hours due to new cells forming on the gust fronts of the mature storm cells.

8.5.3 Ordinary Multicellular Storms in Moderate to Strong Shear. In moderate to strong shear, an ordinary multicellular storm consists of an organized group of cells that develop and move in a consistent manner (Figure 8-9). Typically, the storm contains two to four cells at any given time. New cells develop from cloud towers a few kilometers in diameter, rising at 10 to 15 ms^{-1} (19 to 29 kts) in a preferred region on the updraft flank (see cell 3 at time 0 in Figure 8-9). The newly formed cell does not move into the storm complex but rather grows rapidly and becomes the storm center. Meanwhile, the previous cell (cell 2) begins to decay while another (cell 4) forms. New cells continue to form in this way at intervals of 5 to 15 minutes and each cell is identifiable on radar for about 40 minutes. A total of 30 or more cells may develop during a typical storm's lifetime.

The evolution of one of the cells (cell 3) is depicted by the vertical sections at the bottom of Figure 8-9. The first echo appears in the mid troposphere about 10 minutes after the associated daughter cloud starts rising rapidly. Soon afterward, the echo develops an inverted cup-like shape, partially encompassing a WER that lasts for several minutes until the entire echo has descended to the ground. The WER is associated with a moderately strong updraft reaching 20 to 30 ms^{-1} (39 to 58 kts) before diminishing with the descent of precipitation through it. The storm, as a whole, propagates to the right of the mean troposphere wind.

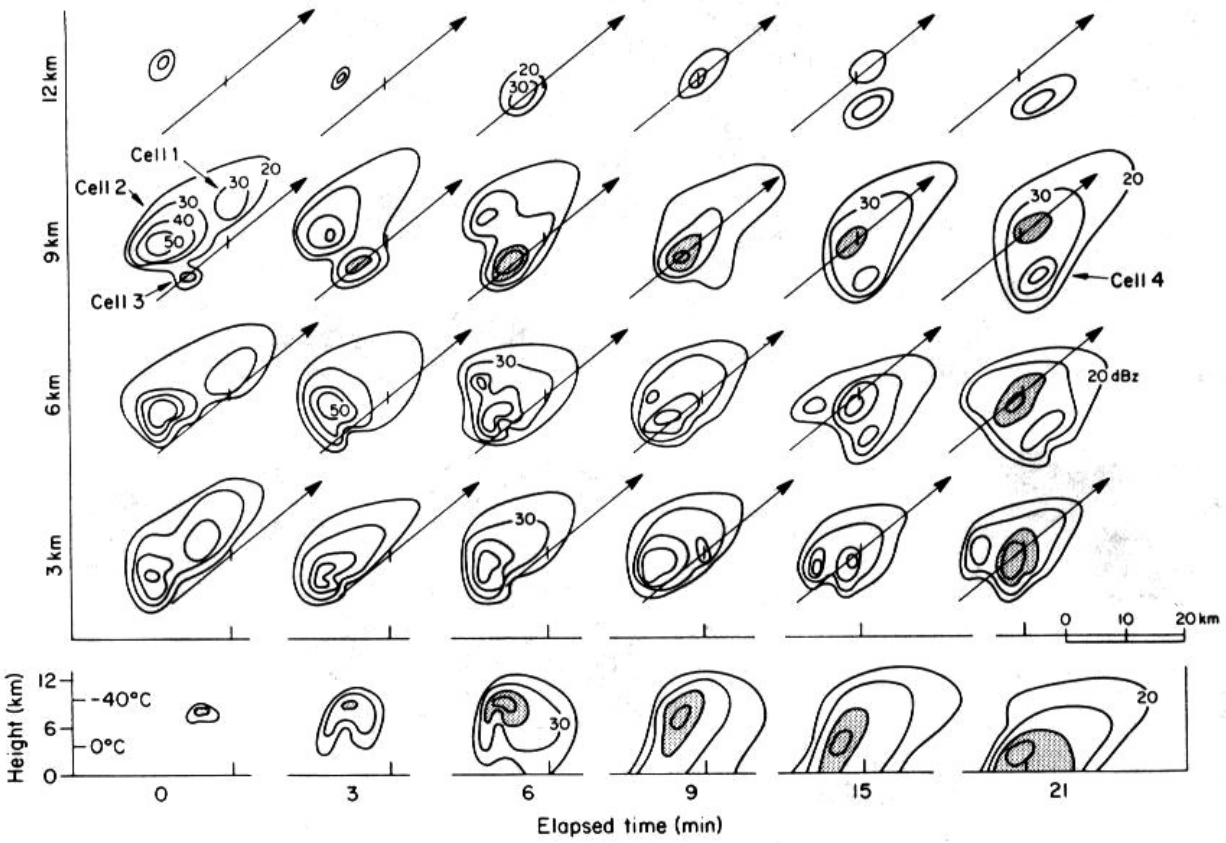

Figure 8-9
Schematic Horizontal and Vertical Radar Sections for an Ordinary Multicell Storm

Various stages during a storm's evolution showing reflectivity contours at 10 dBZ intervals. Horizontal sections are illustrated for four altitudes (3, 6, 9, and 12 km AGL) at six different times. The arrow superimposed on each section depicts the direction of cell motion and is also a geographical reference line for the vertical sections at the bottom of the figure. Cell 3 is shaded to emphasize the history of an individual cell and the vertical cross-sections are also of cell 3 (Chisholm and Renick 1972).

Often in an environment with at least moderate shear, there are storms that appear to be hybrids between ordinary multicellular cluster storms and supercells. These storms have been labeled as weak evolution storms that gradually evolve from their initial multicellular state to the hybrid or weakly evolutionary supecells (Foote and Frank 1983). While individual small cells remain identifiable for brief periods as perturbations, these storms also develop supercelluler characteristics such as a deep persistent mesocyclone that move to the right (or left for mesoanticyclonic storms) of the mean environmental wind (Vasiloff et al. 1986). The majority of supercells have multiple cells, although one cell dominates.

Note that for the sake of the following discussion we are considering the CL supercell storm. We have already mentioned the spectrum of supercell storms including the CL, HP and LP supercell storms. However we have not considered that the Classic in particular also comes in the form of smaller and even very small storms called "mini-supercells" that are much smaller in all dimensions but can be just as severe (Figure 8-10). The "low-topped" supercell is similar except for other than having a shallower depth; other dimensions may be larger than the mini. The low-topped supercells may exhibit wide mesocyclones, and similarly, high-topped supercells may contain narrow mesocyclones. By definition, a mini-supercell is one with the depth and width substantially reduced and includes a narrow mesocyclone.

Low topped and mini supercells can reach anywhere from 20-30 kft (6.1–9.1 km) AGL. Mesocyclone diameters in mini-supercells typically are less than 3 nm (5.6 km). There are no structural differences between low topped, mini, and the more typical large supercells. There are differences in the expected severe weather. Giant hail (>2", 5 cm) is rare because of limited updraft depth, strength, and smaller dimensions. Poor radar sampling of small mesocyclones means that it is more difficult to measure high rotational velocities even when the circulations are relatively near the radar. To illustrate the variability of supercell size, the main supercell in each panel of Figure 8-10 is tornadic, yet only the largest supercell (right panel) was large enough for the radar mesocyclone algorithm to resolve the circulation as a mesocyclone. Therefore, it is important to recognize mini-supercells and be more sensitive to the fact that weak circulations (rotation less than 30 kts (15 ms^{-1})) can carry a significant tornado risk (Grant and Prentice 1996). Moreover, it is important to realize that the limitations of radar, primarily those dealing with beamwidth and aspect ratio and radar horizon, will often prevent the identification of mini-supercells at even modest ranges (greater than about 45 nm (83 km)).

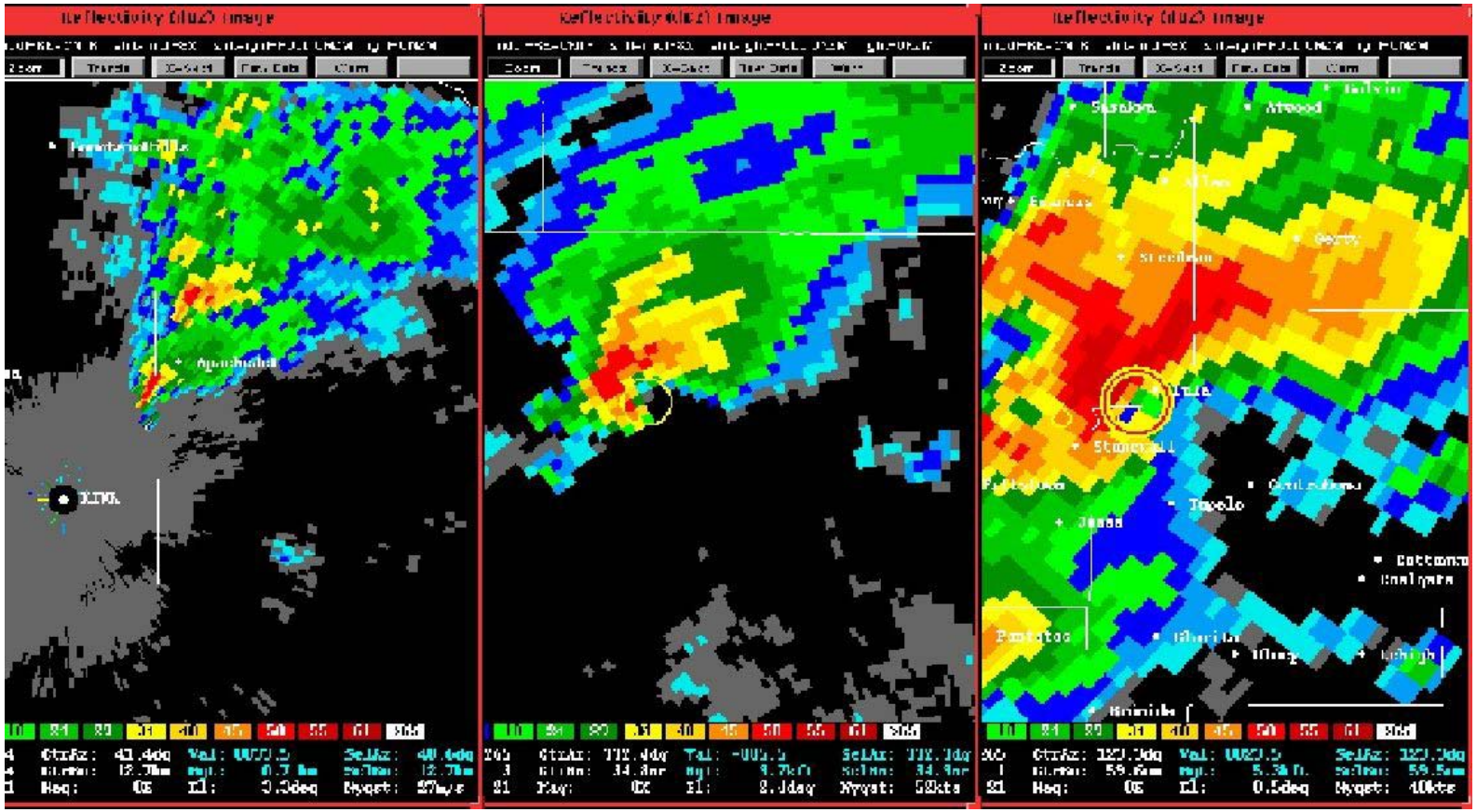

Figure 8-10
Reflectivity Imagery of Supercell Storms

All of these WSR-88D Reflectivity products are the same scale and all are severe, supercell storms. A mini-supercell is pictured left; a mini/low-topped supercell is at the center, and a large, classic supercell, at the right. Note the typical "V-notch" in the upper right of each echo in the 35 dBZ - 40 dBZ echo contours. The red ring in the two right panels indicates a mesocyclone detection by the Mesocyclone Algorithm (WDSS display).

8.5.4 Isolated Supercell Storms. Supercell storms display some basic and persistent characteristics that are often strikingly similar from storm to storm. These characteristics are as follows for a CL type supercell:

1. An approximately elliptic horizontal cross section aloft, often larger in all dimensions than the typical non-severe storm (Figures 8-2a through c). These storms are often characterized by a down-shear "V-notch" or "winged" appearance (Figure 8-10). An extensive plume is observed on radar and this forms part of a much larger visible anvil that extends downstream from the main storm core aloft. At low levels, the echo is situated mainly on the storm's left flank coincident with the forward flank downdraft but the echo may extend toward the right in the form of a hook-shaped appendage that is located mainly in the region of the rear flank downdraft.

2. A persistent WER/BWER is found on the updraft flank. A WER is very common for most supercells, even those with weak mesocyclones. A WER is persistent, and capped by high reflectivities (>45 dBZ) above. The WERs not overlaid by strong reflectivities imply weak or no updraft, such as an overspreading, down-shear, anvil layer. The WER is immediately adjacent to the low-level reflectivity core and bounded with high reflectivity gradients and on the storm-relative low-level inflow side.

   The BWER is less common but may also develop within the WER of the supercell. The BWER is conically shaped and decreases in width with height, extending to a height one-half to two-thirds of the storm depth. The BWER is indicative of a broad, strong (25 to perhaps 60 ms^{-1}; 49 to 115 kts) updraft that contains small cloud particles but little precipitation (Figures 8-11a through c). The storm top is located directly over the BWER and is over the updraft storm flank. When the storm is at moderate to long distances the BWER may not be detectable.

3. A high-reflectivity core (the hail zone) extending all the way to the ground borders the BWER on its left and rear flank resulting in a strong reflectivity gradient there. The largest hailstones are typically located in the strong reflectivity gradient next to the BWER, with smaller hail and rain at increasing distances to the left and left forward of the BWER. This is a size sorting effect associated with the descent of hail within rising air that is also flowing toward the storm's left flank.

   The precipitation cascade downdraft owes its existence to precipitation falling out of the tilted updraft and evaporating in the midlevel stream of environmental air that enters the storm on the right flank (Figure 8-11). However, the primary downdraft, the RFD, is along the storm rear flank and extending into the hook echo. The RFD has proven to be crucial to the production of tornadoes but its origin is still unknown.

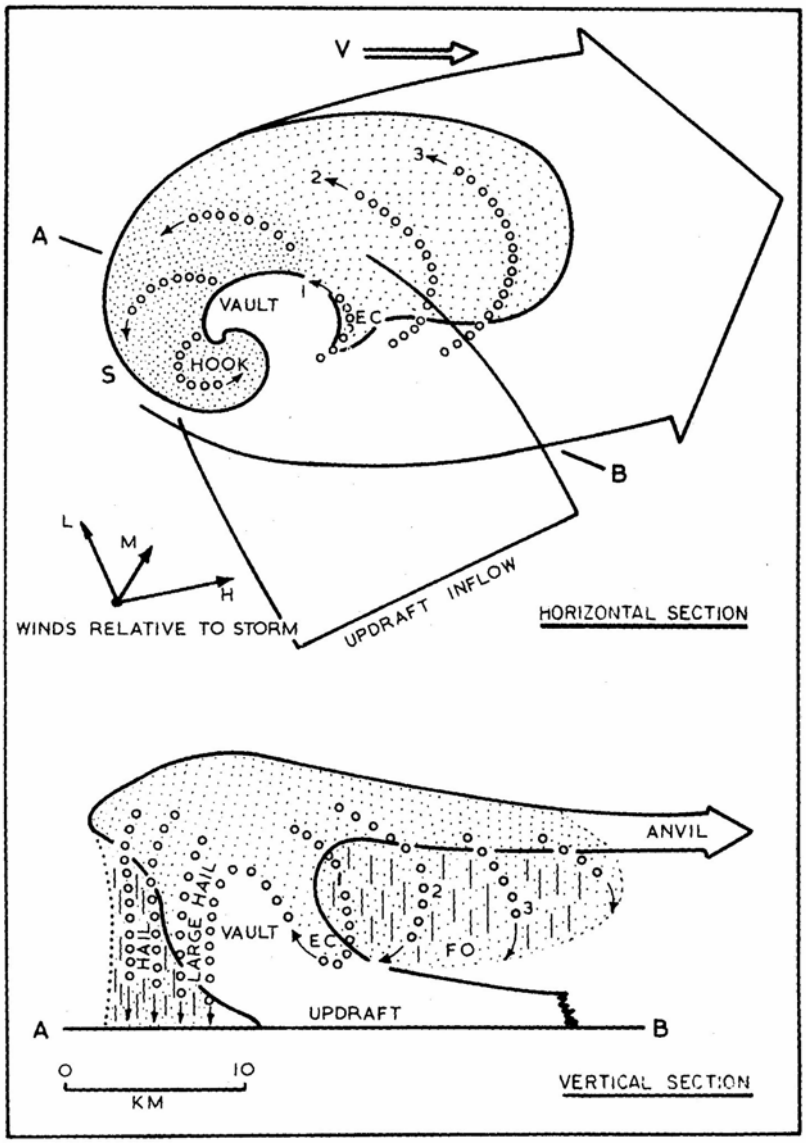

Figure 8-11a
Supercell Storm Illustration - Horizontal and Vertical Sections

Horizontal and vertical sections illustrating relation of updraft to the radar echo in Classic Supercell storm. Solid curves: extent of the updraft air; dotted curves: trajectories of some precipitation particles accounting for the characteristic shape of the radar echo. Horizontal section: light and heavily stippled shading denotes extents of rain and hail in the lower troposphere, respectively; AB oriented in the direction of the mean tropospheric wind shear, into which the updraft is inclined at low levels. Vertical section: broken vertical hatching denotes downdrafts. Characteristic features of the echo pattern referred to in the text are the BWER, hook, and forward overhang (FO) (Browning 1986).

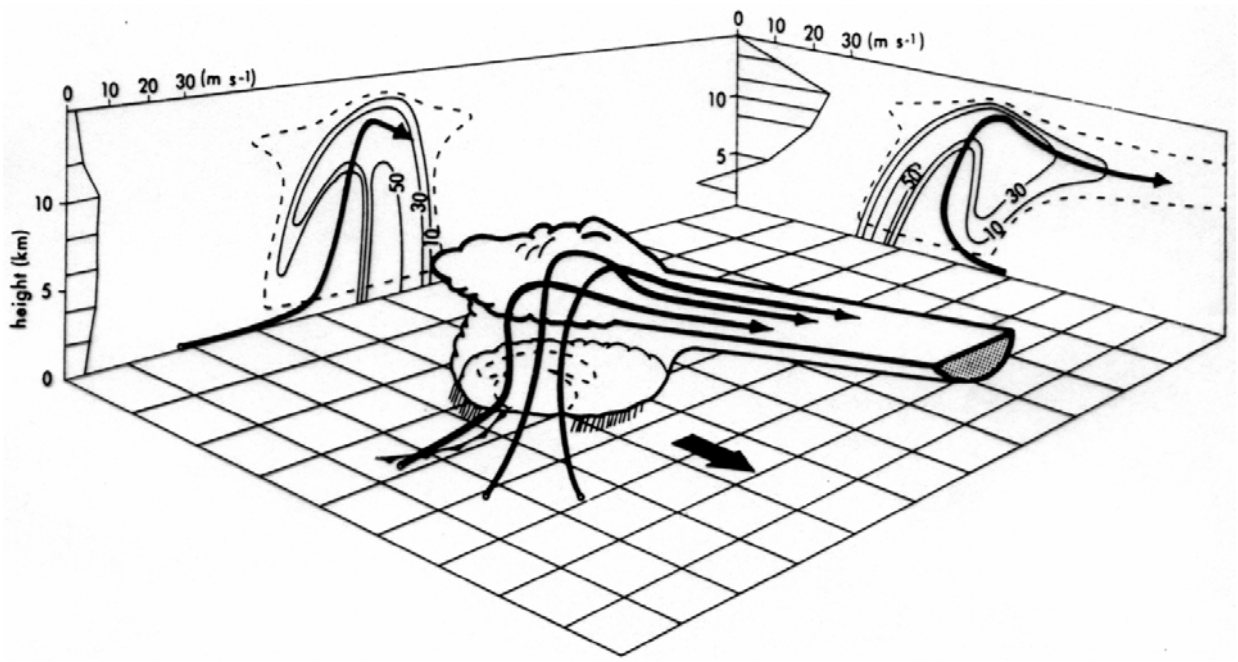

Figure 8-11b
Supercell Storm Illustration - Perspective View

A perspective view of a supercell storm depicting storm airflow and reflectivity structure (Chisholm and Renick 1972). The reflectivity contours are 10, 30, and 50 dBZ.

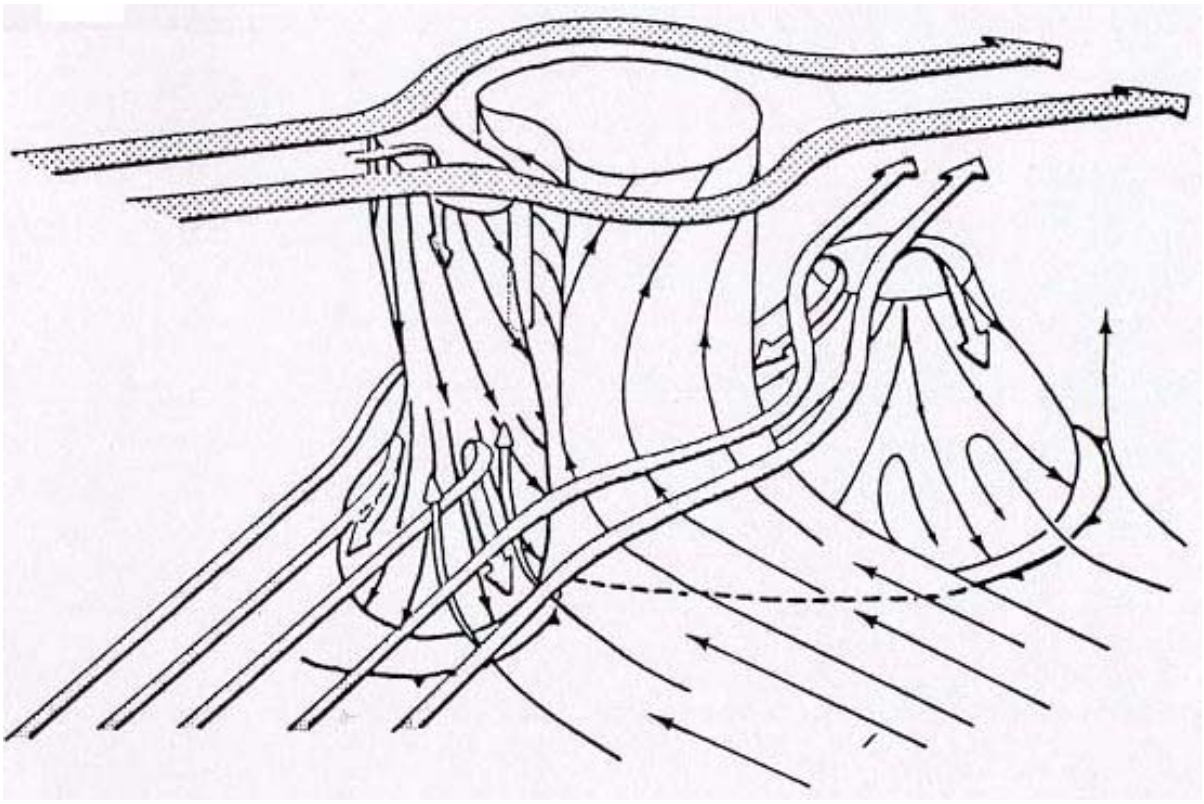

Figure 8-11c
Classic Supercell Storm Draft and Flow Illustration – Three-Dimensional Model.

Model schematic depiction of the drafts, tornado, and mesocyclone in an evolving CL supercell storm. Low-level flow is seen approaching the storm from the right front flank and rising and turning within the updraft in a cyclonic manner. Mid-level flow is shown approaching the storm from the right rear and flowing around the updraft region. A portion of the flow is shown descending into the RFD and the forward flank downdraft (FFD). While high-level flow is depicted as being involved in the RFD that is now in question. Its height of origin and the cause of the associated forcing is unknown at this time. Flow lines throughout the figure are storm relative and conceptual only, not intended to represent flux, streamlines, or trajectories. Conventional frontal symbols are used to denote outflow boundaries at the surface. From Lemon and Doswell (1979).

4. An important period in the life cycle of the CL is the collapse phase. During this phase the echo top lowers, the BWER and WER disappear or are reduced, reflectivity and VILs often decrease, and the hook echo often “wraps up” and disappears. The echo then resembles the ordinary cell, rather than the supercell. While hail size decreases during this period the storm is often undergoing tornadogenesis and producing downburst and microburst winds. The tornado, if it develops, will often reach its maximum size and strength. After collapse, the storm often resembles a typical multicell cluster storm, but may recycle and become a reinvigorated supercell.

The typical visual appearance of an isolated Classic supercell storm is illustrated by Figure 8-2c. For sake of clarity not all features are included, such as the spiraling rain curtain that gives rise to the hook on radar.

The relatively rarer “Left moving” supercell is almost a mirror image to the Classic supercell; thus its “mesocyclone” rotates anticyclonically and can be called a “mesoanticyclone.” The "mirror" is in a vertical plane, parallel to the mean shear vector. Left moving storms often (but not necessarily) move faster and to the left of the mean wind and are notorious "hailers" but usually do not produce tornadoes, in contrast to most CL and HP supercell storms that commonly produce all forms of severe weather.

8.5.5 High Precipitation (HP) Supercell Storms. High Precipitation supercells may be the most common of all supercells. Admittedly, many of the features or characteristics of HP supercells are subjective in nature. These storms are efficient precipitation producers and often associated with strong downdrafts and outflows as well as very large hail. Large amounts of precipitation are available within these storms to wrap around the mesocyclone, producing large, high reflectivity hook echoes. Occasionally, the RFD gust front associated with the hook is sufficiently intense to generate strong convection along its leading edge. The result is that the strongest core can be behind and to the right of the mesocyclone path. Occasionally, this process leads to supercells being part of a much larger line of storms and they occasionally evolve into bow echoes.

There is a wide variety of possible HP supercell configurations (Figure 8-12). However, they all share traits common to supercells – an echo overhang and WER (sometimes a BWER), a displaced echo top and an inflow concavity, often on the front storm flank.

As with the Classic supercell, the inflow and mesocyclone are well correlated with primary updraft and the RFD and are typically long lived. The mesocyclone with the HP is usually well sampled by radar owing to the high reflectivities in the hook and circulation. But the correlation of the RFD with the precipitation cascade in the HP apparently often lead to a relatively cold RFD. Spotters in the field often have a difficult time observing the mesocyclone area most favorable for tornadogenesis. The updraft with its associated WER and BWER are often on the front storm flank. HP environments typically show more boundary layer moisture than that of LP or even CL. However, high boundary layer moisture is not necessary for HP occurrence. Another possibility

includes low anvil-level, storm-relative flow (<18 ms^{-1}) that apparently sometimes allows precipitation to reseed the updraft, improving precipitation efficiency (Rasmussen and Straka 1998). A Classic supercell can evolve into an HP if it is being seeded by aggressive cells on its flanking line or adjacent storms. HP storms carry all threats of severe weather including strong tornadoes. However, the threats of large hail, damaging winds, and flooding are much larger than the tornado threat**.** Recent findings (Markowski 2001; Markowski et al. 2002) suggest that the RFD must be characterized by positive buoyancy and positive CAPE. Most often the RFD within HP supercells is heavy rain and hail laden and frequently "cold," lacking the needed buoyancy for tornado development.

8.5.6 Low Precipitation (LP) Supercell Storms. The LP supercell storm was identified in the 1970s (Davies-Jones et al. 1976; Burgess and Davies-Jones 1979; Bluestein and Parks 1983). LP supercells are generally dominated by updraft with little precipitation reaching the ground. These storms are visualized by exposed updrafts and translucent to essentially transparent precipitation cores. They have small, less reflective and benign-looking radar echoes; produce little precipitation at the ground; lack a rain-cooled downdraft; and the updraft lies behind the radar echo at low levels (Figures 8-13 and 8-14). The relative lack of precipitation leads to poor downdraft development and thus these storms could be said to be outflow deficient. LP supercell updrafts often show significantly midlevel mesocyclones. However, low-level mesocyclones are rare owing to the lack of a well defined RFD. There is rarely a hook echo detected unless the radar is very near the storm, and most of the precipitation is carried well downstream of the updraft by the storm-relative upper-level winds. Maximum reflectivities in LP storms can be weak (< 50 dBZ), however, the reflectivity maximum likely consists of a few large hailstones.

Low Precipitation supercells require significant instability and shear; however, other conditions help to reduce precipitation efficiency. Relatively shallow moisture and abundant dry air aloft reduce available moisture and add to entrainment. However, LP storms can also exist where boundary layer moisture is high. Additionally, very high storm-relative anvil-layer winds (>30 ms^{-1}) transport rising hydrometeors well away from the updraft before they descend from the anvil (Rasmussen and Straka 1998). Hydrometeors may have little chance of recycling back into the updraft, especially if the mid-levels are dry. LP storms are severe and produce large hail and, although rare, can produce weak to moderate tornadoes while appearing innocuous on radar. Significant tornadoes appear to be rare but they have occurred (Burgess and Davies-Jones 1979). LP storms that move into a region of deeper, low-level moisture may transform gradually into CL or even HP supercell storms.

8.5.7 Squall Lines and Mesoscale Convective Systems (MCS). Most occurrences of multicell storms are in the form of clusters and of squall lines (both mid-latitude and tropical), but MCSs also contain multicell characteristics (e.g., convective storms with large stratiform rain regions). Some MCSs' and the related squall line's unique nature of storm structure is based on the environmental conditions and longevity that tend to influence evolution of these large convective systems. This topic has been considered in some detail in the previous chapter (Part B, Chapter 7, of this Handbook) and, thus, will not be covered here.

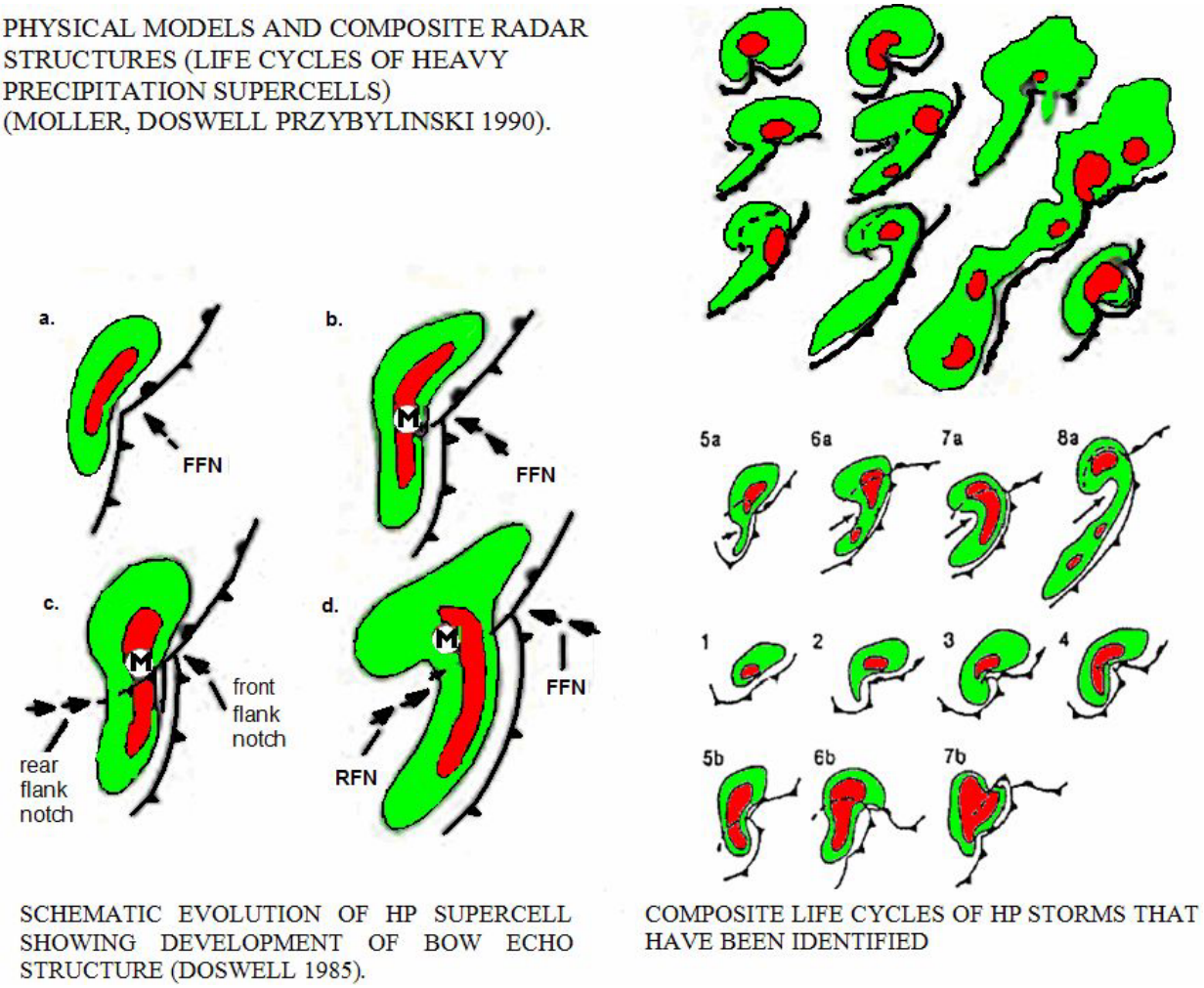

Figure 8-12
A Variety of Documented HP Supercell Reflectivity Configurations

Adapted from Moller et al. 1990 and Doswell 1985.

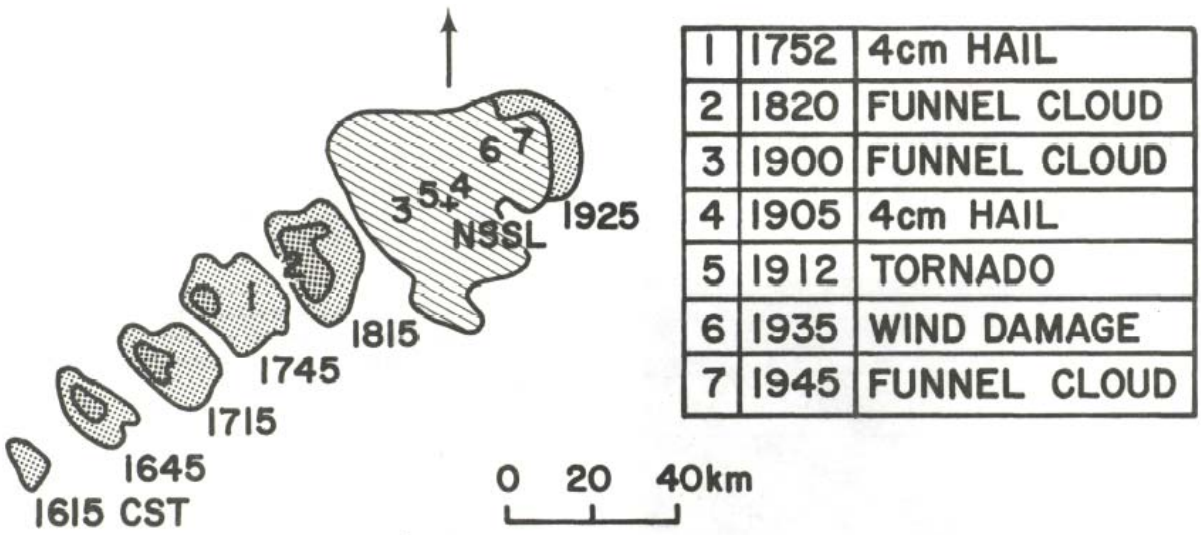

1	1752	4cm HAIL
2	1820	FUNNEL CLOUD
3	1900	FUNNEL CLOUD
4	1905	4cm HAIL
5	1912	TORNADO
6	1935	WIND DAMAGE
7	1945	FUNNEL CLOUD

Figure 8-13
Radar Chronology of an LP Storm

Radar chronology of an LP storm and a list of severe weather events associated with that storm. Reflectivity contour values are 20 and 40 dBZ, respectively. Hatching represents ground clutter (from Davies-Jones et al. 1976).

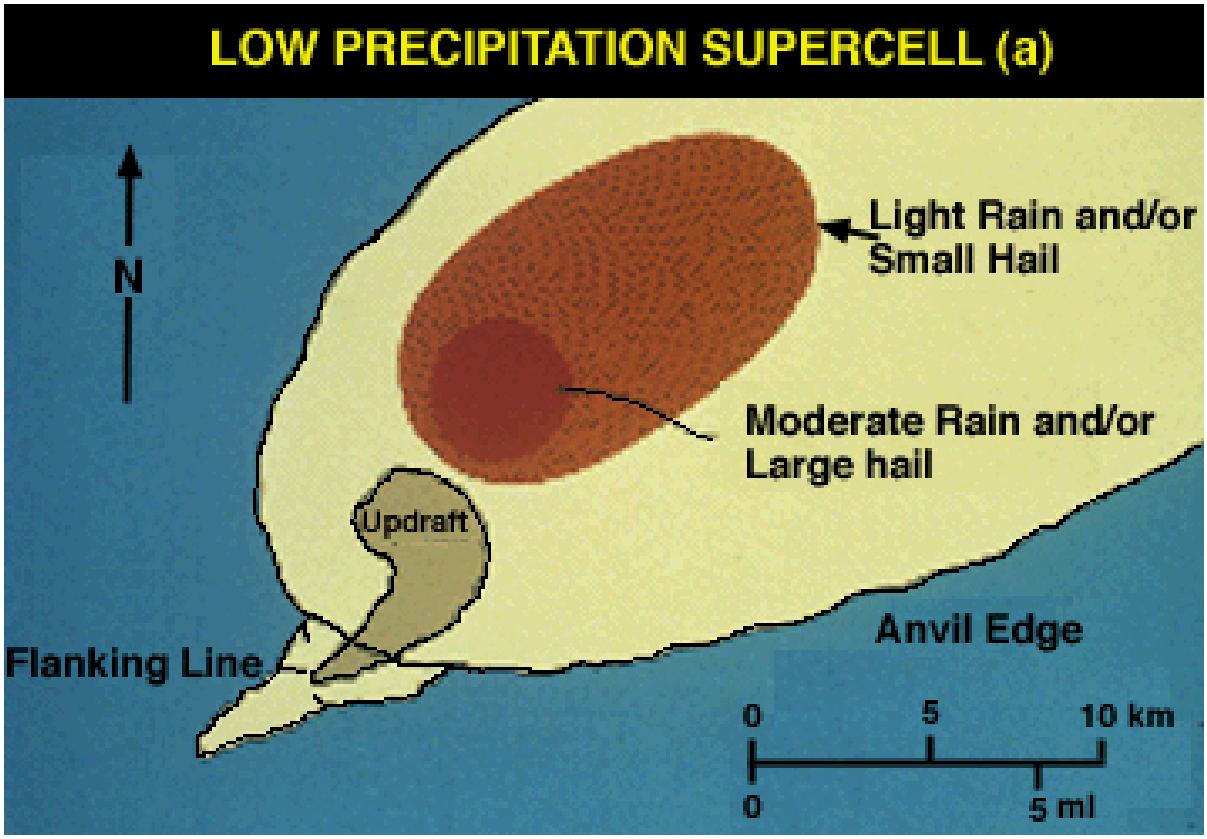

(Reproduced/modified by permission of American Geophysical Union.)

Figure 8-14
Top View of an LP Supercell

Low Precipitation supercell schematic. (After Doswell and Burgess 1993)

8.5.8 Transformation From One Type of Storm to Another. Deep convection frequently begins in mid-afternoon as isolated ordinary storms, some of which evolve into severe multicell cluster or supercell storms. Often more storms form, their outflows combine into a large cold pool and resulting gust front, and a squall line of ordinary cells eventually develops. However, even these squall lines that take on an appearance of a two-dimensional quasi-linear system can also become tornadic. Godfrey et al. (2004) found that these tornadic systems tend to occur when the environment is characterized by strong low-level bulk shears and high low-level CAPE. Supercells generally end their lives by reverting to an ordinary multicellular state or by becoming an ordinary member of a squall line. LP storms may evolve into CL supercells if they move into a more moist environment, but many dissipate in the LP state or occasionally merge into squall lines.

Occasionally, a reverse transformation takes place with a solid squall line of ordinary cells evolving into a short line of a few very intense supercells. In one well-documented case, this transformation occurred after dark as an intense short wave trough aloft overtook the squall line. The resulting supercells produced violent and deadly tornadoes (Burgess and Curran 1985).

The collapse phase of a supercell storm, including those associated with MCSs, is often accompanied with severe winds due to strong downdrafts or downbursts and, perhaps, strong tornadoes. This stage is marked by a dramatic weakening or overall collapse of a portion of the main updraft and greatly enhanced downdrafts (Lemon and Doswell 1979; Dowel and Bluestein 2000). On radar, it can be recognized by sharp declines in storm top, maximum reflectivity aloft, and vertical extent of the WER or BWER (Lemon and Doswell 1979; Dowel and Bluestein 2002a, b). However, as the reflectivity structure weakens, the low-level mesocyclone is strengthening with amplifying rotational velocities. Thus, to discriminate this collapse phase from a true general weakening of the storm, the mesocyclone is revealed by the velocity data to be intensifying. In fact, the TVS, if within range, may also be detected at this time.

8.5.9 Additional Information. For more information on the subject of severe convective storms and their operational identification, the reader is referred to Part D, Chapter 4 and Part B, Chapter 7, of this Handbook and the following web sites.

Warning Decision Training Branch – Courses & Workshops

http://www.wdtb.noaa.gov/courses/index.html

Warning Decision Training Branch – Distance Learning Operations Course

http://www.wdtb.noaa.gov/DLCourses/dloc/dlocmain.html

University of Illinois Dept. of Atmos. Sciences – Severe Storms: Online Meteorology Guide

http://ww2010.atmos.uiuc.edu/(Gh)/guides/mtr/svr/home.rxml

REFERENCES

Bluestein, H. B., and C. R. Parks, 1983: A synoptic and photographic climatology of low-precipitation, severe thunderstorms in the southern plains. *Mon. Wea. Rev*., **111,** 2034-2046.

Brady, R. H., and E. Szoke, 1988: The landspout--a common type of northeast Colorado tornado. Preprints, *15th Conf. on Severe Local Storms*, Baltimore, MD, Amer. Meteor. Soc., 312-315.

Brooks, H. E., J. W. Lee, and J. P. Carven, 2003: The spatial distribution of severe thunderstorm and tornado environments from global reanalysis data. Atmospheric Research, pp. 67-68 and 73-94.

Brown, R. A., L. R. Lemon, and D. W. Burgess, 1978: Tornado detection by pulsed Doppler radar. *Mon. Wea. Rev*., **106,** 29-38.

Browning, K. A., 1964: Airflow and precipitation trajectories within severe local storms which travel to the right of the winds. *J. Atmos. Sci*., **21,** 634-639.

Browning, K. A., 1977: The structure and mechanism of hailstorms. *Hail: A Review of Hail Science and Hail Suppression, Meteor. Monogr.,* Amer. Meteor. Soc., **16,** 1-43.

Browning, K. A., 1986: General circulation of middle-latitude thunderstorms. *Thunderstorm Morphology and Dynamics*, E. Kessler (Ed). Univ. of Oklahoma Press, Norman, OK, pp. 133-152.

Burgess, D.W., 1974: Study of a right-moving thunderstorm utilizing new single Doppler radar evidence. M. S. Thesis, Dept. of Meteorology, Univ. of Oklahoma, 77 pp.

Burgess, D. W., 1976: Single Doppler radar vortex recognition: Part I Mesocyclone signatures. Preprints, *17th Conf. on Radar Meteorology*, Seattle, WA, Amer. Meteor. Soc., 97-103.

Burgess, D. W., and R. P. Davies-Jones, 1979: Unusual tornadic storms in eastern Oklahoma on 5 December 1975. *Mon. Wea. Rev*., **107,** 451-457.

Burgess, D. W., V. T. Wood and R. A. Brown, 1982: Mesocyclone evolution statistics. Preprints, *12th Conf. on Severe Local Storms, San Antonio, TX,* Amer. Meteor. *Soc*., 422-424.

Burgess, D. W., and E. B. Curran, 1985: The relationship of storm type to environment in Oklahoma on 26 April 1984. Preprints, *14th Conf. on Severe Local Storms*, Indianapolis, IN, Amer. Meteor. Soc., 208-211.

Burgess, D. W., and P. S. Ray, 1986: Principles of radar. Chapt. 6, Mesoscale Meteorology and Forecasting, P.S. Ray, (Ed), Amer. Meteor. Soc., 85-117.

Byers, H. R., and R. R. Braham. 1949: *The Thunderstorm*. U.S. Govt. Printing Office, Washington, D.C, 287 pp.

COMET, 1996: Anticipating Convective Storm Structure and Evolution and A Convective Storm Matrix: Buoyancy/Shear Dependencies, Cooperative Program for Operational Meteorology, Education and Training, Distance Learning Program. http://www.meted.ucar.edu/convectn/mcs/.

Chisholm, A. J., and J. H. Renick, 1972: The kinematics of multicell and supercell Alberta hailstorms. Alberta Hail Studies, 1972, Research Council of Alberta Hail Studies, Rep. No. 72-2, 24-31.

Davies-Jones, R. P., D. W. Burgess, and L. R. Lemon, 1976: An atypical tornado-producing cumulonimbus. *Weather*, **31,** 336-347.

Davies-Jones, R. P., 1982: Tornado interception with mobile teams. *Instruments and Techniques for Thunderstorm Observation and Analysis,* E. Kessler, (Ed). U.S. Govt. Printing Office, pp. 33-46.

Davies-Jones, R. P., 1984: Streamwise vorticity: The origin of updraft rotation in supercell storms. *J. Atmos. Sci*., **41,** 2991-3006.

Davies-Jones, R. P., 1986: Tornado dynamics. *Thunderstorm Morphology and Dynamics*, E. Kessler, (Ed). Univ. of Oklahoma Press, pp. 197-236.

Doswell, C. A. III, 1985: The operational meteorology of convective weather. Vol. II: Storm scale Analysis. NOAA Tech. Memo. ERL ESG-15, 240 pp.

Doswell, C. A. III, and D. W. Burgess, 1993: Tornadoes and tornadic storms. A review of conceptual models. *The Tornado: Its Structure, Dynamics, Hazards, and Prediction,* (C. Church et al, Eds), Geophys. Monogr. 79, Amer. Geophys. Union, 161-172.

Doswell, C. A. III, 2001, Severe convective storms – An overview. Severe Convective Storms, *Meteor. Monogr.*, ***50,*** Ed. C. A. Doswell, Amer. Meteor. Soc., Boston, MA, pp. 1-26.

Dowell, D. C., and H. B. Bluestein, 2000: Conceptual models of cyclic supercell tornadogenesis. Preprints*, 20th Conf. on Severe Local Storms*, Orlando, FL, Amer. Meteor. Soc., 259-262.

Dowell, D. C., and H. B. Bluestein, 2002a: The 8 June 1995 McLean, Texas, Storm. Part II: Cyclic Tornado Formation, Maintenance, and Dissipation, *Mon. Wea. Rev.*, **130**, 2649-2670.

Dowell, D. C., and H. B. Bluestein, 2002b: The 8 June 1995 McLean, Texas, Storm. Part I: Observations of Cyclic Tornadogenesis, *Mon. Wea. Rev.*, **130**, 2626-2648.

Foote, G. B. and H. W. Frank, 1983: Case study of a hailstorm in Colorado. Part III: Air flow from triple-Doppler measurements. *J. Atmos. Sci*., **40,** 686-707.

Godfrey, S., R. J. Trapp, H. E. Brooks, 2004: A study of the pre-storm environment of tornadic quasi-linear convective systems. Preprints*, 22th Conf. on Severe Local Storms*, Hyannis, MA, Amer. Meteor. Soc., 259-262.

Fujita, T. T., 1978: Manual of downburst identification for Project NIMROD. SMRP Res. Pap. 156, University of Chicago, 104 pp.

Fujita, T. T., 1985: *The Downburst*. Satellite and Mesometeorology Research Project. Research Paper No. 210, University of Chicago, 122 pp.

Grant, B. N., and R. Prentice, 1996: Mesocyclone characteristics of mini supercell thunderstorms. Preprints, *15th Conf. on Wea. Anal. and Forecasting*, Norfolk, VA, Amer. Meteor. Soc., 362-365

Johns, R.. H., J. M. Davies, and P. W. Leftwich, 1993: Some wind and instability parameters associated with strong and violent tornadoes. 2. Variations in the combinations of wind and instability parameters. *The Tornado: Its Structure, Dynamics, Hazards, and Prediction* (Geophys. Monogr. 79) (C. Church, D. Burgess, C. Doswell, and R. Davies-Jones, Eds.), Amer. Geophys. Union, 583-590.

JDOP Staff, 1979: Final Report on Joint Doppler Operational Project (JDOP) 1976-1978. NOAA Tech. Memo. ERL NSSL-86, 84 pp.

Klemp, J. B. 1987: Dynamics of tornadic thunderstorms. Annual Reviews Fluid Mechanical, 19, 369-402.

Lemon, L. R., 1980: Severe thunderstorm radar identification techniques and warning criteria. NOAA Tech. Memo. NWS NSSFC-3, 60 pp.

Lemon, L. R., and C. A. Doswell, III, 1979: Severe thunderstorm evolution and mesocyclone structure as related to tornadogenesis. *Mon. Wea. Rev*., **107**, 1184-1197.

Lemon, L. R., 1998: Updraft identification with radar. Preprints, *19th Conf. on Severe Local Storms*, Minneapolis, MN, Amer. Meteor. Soc., 709-712.

Maddox, R. A., 1976: An evaluation of tornado proximity wind and stability data. *Mon. Wea. Rev*., **104**, 33-142.

Markowski, P. M., 2002: Hook echoes and rear-flank downdrafts: A review. *Mon. Wea. Rev*., **130**, 852-876.

Markowski, P. M., J. M. Straka, and E. N. Rasmussen, 2002: Direct surface thermodynamic observations within the rear-flank downdrafts of nontornadic and tornadic supercells. Mon. Wea. Rev., **130,** 1692-1721.

Marwitz, J. D., 1972: The structure and motion of severe hailstorms. Part III: Severely sheared storms. *J. Appl. Meteor*., **11,** 189-201.

Moller, A.R., C.A. Doswell III and R. Przybylinski, 1990: High-precipitation supercells: A conceptual model and documentation. Preprints, *16th Conf. on Severe Local Storms,* Kananaskis Park, AB, Amer. Meteor. Soc., 52-57.

NOAA, 1980: Tornado: A Spotter's Guide (Slide series supplement to movie). Available from Weather and Flood Warnings Coordination Program. NWS, NOAA, Silver Spring, MD.

Rasmussen, E. N.**,** and J. M. Straka, 1998: Variations in supercell morphology. Part I: Observations of the role of upper-level storm-relative flow. *Mon. Wea. Rev.*, **126**, 2406-2421.

Vasiloff, S. V., E. A. Brandes, R. P. Davies-Jones, and P. S. Ray, 1986: An Investigation of the transition from multicell to supercell storms. J. Climate Appl. Meteor., **25,** 1022-1036.

Witt, A., and S. P. Nelson, 1984: The relationship between upper-level divergent outflow magnitude as measured by Doppler radar and hailstorm intensity. Preprints*, 22nd Conf. on Radar Meteorology*, Zurich, Amer. Meteor. Soc., 108-111.